NASA TECHNICAL NOTE

NASA TN D-6943

NASA TN D-6943

FLIGHT MEASUREMENTS OF BUFFET CHARACTERISTICS OF THE F-104 AIRPLANE FOR SELECTED WING-FLAP DEFLECTIONS

by Edward L. Friend and Walter J. Sefic

Flight Research Center
Edwards, Calif. 93523

NATIONAL AERONAUTICS AND SPACE ADMINISTRATION • WASHINGTON, D. C. • AUGUST 1972

1. Report No. NASA TN D-6943	2. Government Accession No.	3. Recipient's Catalog No.
4. Title and Subtitle FLIGHT MEASUREMENTS OF BUFFET CHARACTERISTICS OF THE F-104 AIRPLANE FOR SELECTED WING-FLAP DEFLECTIONS		5. Report Date August 1972 6. Performing Organization Code
7. Author(s) Edward L. Friend and Walter J. Sefic		8. Performing Organization Report No. H-666 10. Work Unit No. 136-63-03-00-24
9. Performing Organization Name and Address NASA Flight Research Center P. O. Box 273 Edwards, California 93523		11. Contract or Grant No. 13. Type of Report and Period Covered Technical Note
12. Sponsoring Agency Name and Address National Aeronautics and Space Administration Washington, D. C. 20546		14. Sponsoring Agency Code
15. Supplementary Notes		

16. Abstract

A flight program was conducted on the F-104 airplane to investigate the effects of moderate deflections of wing leading- and trailing-edge flaps on the buffet characteristics at subsonic and transonic Mach numbers. Selected deflections of the wing leading- and trailing-edge flaps, individually and in combination, were used to assess buffet onset, intensity, and frequency; lift curves; and wing-rock characteristics for each configuration. Increased deflection of the trailing-edge flap delayed the buffet onset and buffet intensity rise to a significantly higher airplane normal-force coefficient. Deflection of the leading-edge flap produced some delay in buffet onset and the resulting intensity rise at low subsonic speeds. Increased deflection of the trailing-edge flap provided appreciable lift increments in the angle-of-attack range covered, whereas the leading-edge flap provided lift increments only at high angles of attack. The pilots appreciated the increased maneuvering envelope provided by the flaps because of the improved turn capability.

17. Key Words (Suggested by Author(s)) Flight buffet characteristics Buffet characteristics	18. Distribution Statement Unclassified - Unlimited		
19. Security Classif. (of this report) Unclassified	20. Security Classif. (of this page) Unclassified	21. No. of Pages 47	22. Price* $3.00

* For sale by the National Technical Information Service, Springfield, Virginia 22151

FLIGHT MEASUREMENTS OF BUFFET CHARACTERISTICS OF THE F-104 AIRPLANE FOR SELECTED WING-FLAP DEFLECTIONS

Edward L. Friend and Walter J. Sefic
Flight Research Center

INTRODUCTION

The maneuverability and performance of fighter aircraft at high subsonic speeds and high-lift flight conditions are usually degraded by the effects of wing flow separation. One of the first effects of flow separation is airframe buffeting. The reduction in the buffet boundaries as Mach number increases, which occurs with many aircraft configurations, is discussed in reference 1. In response to military requirements for improved maneuvering flight capability, many flight and wind-tunnel studies have been made to investigate the factors which influence buffeting. Some of the first wind-tunnel studies indicated that buffet could be alleviated or reduced through deflection of wing leading-edge and trailing-edge flaps, and, as reported in references 2 to 4, through the use of advanced airfoil shapes. Some early flight results on two wing planform configurations showing improvements due to flap deflection are reported in references 5 and 6.

Programs and studies have been undertaken more recently to define the buffet phenomenon for existing airplanes and to improve wind-tunnel techniques for predicting buffet onset and buffet intensity through correlation of flight and wind-tunnel characteristics. Included in the flight studies are the detection and definition of variations in stability and control and overall performance during tracking tasks.

At present, full-scale flight testing appears to be the most effective means of fully assessing measures to alleviate buffeting. As an extension of an earlier NASA flight investigation of buffet characteristics (ref. 7), a flight program was conducted to investigate the effects of wing leading- and trailing-edge flap configurations on buffet characteristics of several aircraft. A preliminary summary of this investigation was reported in reference 8 and at the AIAA Atmospheric Flight Mechanics Conference, Tullahoma, Tenn., May 13 to 15, 1970. References 1 to 3 also present some results from this buffet study.

This report provides additional flight data and a more comprehensive analysis of the effects of wing-flap deflection on the F-104 airplane than were included in reference 8. Results are shown in terms of buffet onset, intensity, and frequency; lift curves; and associated pilot comments as they relate to airplane response and handling for many wing-flap configurations.

SYMBOLS

Physical quantities in this report are given in the International System of Units (SI)

and parenthetically in U. S. Customary Units. The measurements were taken in U. S. Customary Units. Factors relating the two systems are presented in reference 9.

a_n	normal acceleration at airplane center of gravity, g
a_{n_p}	normal acceleration at pilot's compartment, g
B_w	bending moment on wing panel, m-N (in-lb)
C_{N_A}	airplane normal-force coefficient, $\frac{a_n W}{qS}$
g	acceleration due to gravity, m/sec^2 (ft/sec^2)
h_p	pressure altitude, m (ft)
M	Mach number
q	dynamic pressure, N/m^2 (lb/ft^2)
S	area of wing, including fuselage, m^2 (ft^2)
W	airplane gross weight, N (lb)
α	indicated airplane angle of attack, deg
δ_{le}	deflection of leading-edge flap, deg
δ_{te}	deflection of trailing-edge flap, deg
σ	root-mean-square value of buffet component of associated quantity
Φ	power spectral density of associated quantity

TEST VEHICLE

An F-104 airplane was used for this investigation. A three-view drawing of the airplane is shown in figure 1, and the geometry of the wing and wing flaps is shown in figures 2(a) and 2(b). Pertinent dimensions and physical characteristics are given in table 1.

The F-104 is a single-place, high-performance fighter airplane designed to operate at high subsonic cruise and high supersonic combat speeds. Notable features of the airplane include short, straight, extremely thin wings with negative dihedral, a controllable horizontal stabilizer mounted at the top of the vertical stabilizer, and a stick kicker which limits angle of attack. The wings have leading- and trailing-edge flaps, and a boundary-layer control system which is used in conjunction with the trailing-edge flap.

The boundary-layer control system was not activated during the tests.

The trailing-edge flaps are attached to the aft beam of each wing panel between the wing fillets and the inboard end of the ailerons; they are hinged at the forward lower edge. The leading-edge flaps form the leading edge of each wing between the fuselage and the wing-tip fairings; they are hinged at the lower edge. For the buffet program, the wing-flap deflection system was redesigned to provide variable and independent deflection of the wing flaps.

INSTRUMENTATION SYSTEM

Data Acquisition

The airplane was instrumented for measurement of various flight parameters, including airspeed, altitude, angle of attack, angle of wing-flap deflection, normal acceleration near the center of gravity, normal acceleration at the pilot's compartment, and wing bending moment on one wing.

A standard NASA airspeed head (ref. 10) and angle-of-attack vane were installed on a boom mounted on the nose of the airplane. The angle of attack was measured relative to the fuselage reference line. The accelerometer for measuring the steady-state acceleration at the airplane center of gravity was filtered above 4 hertz to eliminate the buffet component. The instrument was at fuselage station 10.69 meters (421 inches) in the upper forward section of the wheel well. The unfiltered normal accelerometer for measuring the buffet loads was in the pilot's compartment on the heavy structure supporting the pilot's seat. The strain gages to measure the wing bending moment were located externally on a wing station (fig. 2) near the wing fuselage fairing and at approximately 38 percent of the wing semispan.

Data Recording and Processing

Data were acquired by a pulse code modulation (PCM) system. This system was composed of an airborne PCM encoder, a telemetry transmitter, and a ground-based telemetry receiver coupled with a tape recorder and display equipment so that a permanent record of the flight data could be obtained in digital form on tape and a real-time analog display record could be viewed during flight. The time display charts were used to determine the flight times for which data would be analyzed and the onset of buffet from the oscillation of the traces, as shown in figures 3(a) and 3(b). Computer programs were used to reduce the raw data from the tape to the desired parameter form. Data were taken at 200 samples per second per channel.

Data Interpretation and Analysis

Typical analog time histories are shown in figures 3(a) and 3(b) including traces of airplane normal acceleration, angle of attack, and wing bending moment taken during the buffet portion of each maneuver. From traces such as these, the onset of buffet and the portion of each maneuver to be analyzed in terms of root mean square and power spectral density were determined.

The normal acceleration and load traces show two kinds of variations during buffeting. One is a slow, steady variation which represents the maneuver component. Superimposed on the slow, steadily varying load traces is a rapidly fluctuating load which represents the buffet load. The initial continuous, rapid fluctuation in the normal acceleration trace (sensor in the pilot's compartment) and the wing bending moment trace was interpreted to indicate the onset of buffet. Buffet-onset conditions were usually found to correlate with a root-mean-square value of approximately ±0.025g. Buffet loads were analyzed in segments during increasing load or angle-of-attack flight conditions. One-second time intervals were chosen for every 1° to 2° of variation in angle of attack during the buffet periods. After the segments to be analyzed were established, computer programs were used to analyze the digital data. First, the buffet loads were separated from the maneuver loads by a numerical filtering technique described in reference 11. Root-mean-square values of the buffet loads for each segment were then established. These values were defined as the buffet loads.

Power spectral techniques were used to indicate the power and frequency distribution of the buffet parameters. Time segments of 3 seconds were chosen for each maneuver at times of high-intensity oscillations and approximately constant angle of attack. This time segment was chosen to confine the analysis to the period of the highest output of the wing sensors and to an interval of fairly constant response. The data were analyzed at 100 samples per second and 40 lags. A numerical technique, described in reference 12, was used to reduce the data to the required form.

Accuracy

The accuracy of the data in terms of the estimated error for the major parameters used in this investigation is as follows:

M	±0.01
h_p	±61 m (±200 ft)
α	±0.50°
q	±100 N/m^2 (±3 lb/ft^2)
$\sigma_{a_{n_p}}$	±0.01 g
W	±1334 N (±300 lb)
C_{N_A}	±0.03
a_n	±0.05g
σ_{B_w}	±90 m-N (±800 in-lb)

Angle-of-attack measurements are presented as indicated data, uncorrected for upwash. An in-flight airspeed calibration provided true Mach number and altitude.

FLIGHT TEST CONDITIONS

Flight tests were made over a range of Mach number for various wing-geometry

configurations. Leading-edge and trailing-edge flaps were deflected independently from 0° to a maximum of approximately 13°, and for various combined settings. The wing-geometry configurations tested and the corresponding Mach number ranges and dynamic pressures are listed in table 2. Test maneuvers were made with an airplane gross weight of approximately 66.7 kilonewtons (15,000 pounds) to 80.1 kilonewtons (18,000 pounds).

During these flight tests, the airplane was generally flown to the angle-of-attack limits established by the stick kicker.

The program was conducted with the tip tanks removed from the airplane. Buffet-onset data were obtained during both windup turns and pushover/pullup maneuvers; however, buffet-intensity data were obtained only in the windup-turn maneuvers.

RESULTS AND DISCUSSION

Buffet Boundaries

Variation of buffet boundary. - The variation of the boundary for buffet onset is shown in figure 4 for selected wing-flap deflections in terms of airplane normal-force coefficient and airplane angle of attack as a function of Mach number. The clean-wing buffet-onset boundary occurs at a relatively low lift level at low subsonic Mach numbers and rises as Mach numbers approach transonic values. The relatively thin, low-aspect-ratio, sharp-leading-edge wing of the F-104 airplane is similar to some supersonic wing configurations which have a low lift level for buffet onset at low subsonic speeds. However, at transonic speeds, supersonic airfoils show relatively high levels of airplane normal-force coefficient prior to the onset of significant boundary-layer shock effects, with a resulting delay in buffet onset. This increased lift level for buffet onset is discussed in references 1 and 13 for the X-15 and X-3 airplanes, respectively.

As shown in figure 4, deflection of the wing flaps in the speed range covered by these tests provided a marked improvement in delaying buffet onset to a higher lift level. Results for the intermediate wing-flap configuration indicated a higher boundary than for the clean-wing configuration but had a similar trend. The highest levels of lift prior to buffet onset were obtained with the maximum wing-flap configuration tested. However, at $M \approx 0.85$ to 0.90 the data show a dip in this boundary curve to lift levels of about the same value as that for the intermediate wing-flap setting. The lift levels shown for buffet onset for the higher wing-flap deflections at subsonic Mach numbers are representative of airplanes with high-aspect-ratio wings with thick, blunt leading edges (ref. 1). Thus, higher loads would be expected to develop at low angles of attack prior to buffet onset.

The decrease and sudden rise in the buffet-onset boundary with the maximum wing-flap configuration at transonic Mach numbers is similar to results for many subsonic wing configurations, although for these tests it did not decrease to as low a lift level.

The maximum depth of buffet penetration is shown in figure 5 in relation to the normal-force-coefficient and angle-of-attack boundaries for buffet onset. In most instances, the penetration shown was terminated at or near the stick kicker limits.

Increased wing-flap deflection substantially improved the absolute level of lift available before the stick-kicker limit was reached, particularly at low subsonic Mach numbers. As Mach number increases, the buffet-onset boundary and the maximum test-condition boundary tend to converge. This trend was due primarily to a power limitation at high Mach numbers, which limited the maximum attainable angle of attack.

Effect of flaps on buffet onset. - The effects of individual and combined deflection of the wing leading- and trailing-edge flaps on the levels of airplane normal-force coefficient for buffet onset at Mach numbers of approximately 0.83 and 0.89 are shown in figure 6. The data for a Mach number of 0.83 (fig. 6(a)) indicate that deflection of the trailing-edge flap is more effective than deflection of the leading-edge flap in delaying buffet onset. The maximum gain in C_{N_A} for buffet onset due to leading-edge flap deflection was approximately 0.1 for the range of trailing-edge flap settings tested. The maximum gain for trailing-edge flap deflection was approximately 0.2 for the range of leading-edge flap deflections tested. In contrast to the results shown for a Mach number of 0.83, the data for a Mach number of 0.89 (fig. 6(b)) indicate that the leading-edge flaps produced slight gains at low deflection angles but had a detrimental effect at the higher angles. Whereas the gain in C_{N_A} for low leading-edge flap deflection was less than 0.1, that for the maximum trailing-edge flap deflection reached about 0.25. The flight results for the F-105F and F-5A airplanes in references 5 and 6 indicate similar trends.

Reference 13 analyzes the buffet characteristics of the X-3 airplane, which had an airfoil configuration similar to that of the F-104 airplane. The analysis shows that as Mach number increases from approximately 0.85 to 0.95, the flow separation pattern changes with increasing angle of attack from separation at the leading edge to separation at both the leading and trailing edges. Similarly, it is believed that separation from the F-104 wing first occurs just back of the leading-edge flap near a Mach number of 0.89. Thus low deflection settings of the leading edge tend to be ineffective in delaying buffet onset at that test condition. Reference 13 also states that larger deflections of a leading-edge flap would result in earlier flow separation on the upper surface at Mach numbers above 0.85 and would probably cause flow separation on the lower surface. The present results for the high leading-edge deflection setting at a Mach number of 0.89 indicate a similar reduction in the value of C_{N_A} at which buffet onset occurs.

Buffet Intensity

Effect of Mach number on buffet loads. - The variation with C_{N_A} of buffet intensity, expressed as root-mean-square values of fluctuating normal acceleration at the pilot's compartment, $\sigma_{a_{n_p}}$, and wing bending moment, σ_{B_W}, is shown in figures 7(a) to 7(c) for three airfoil configurations and a series of subsonic Mach numbers. The slopes of the lines faired through the root-mean-square values of a_{n_p} for the three configurations are generally similar and show a rapid intensity rise with increasing C_{N_A} at all Mach numbers. A small Mach number effect is shown at the higher Mach numbers, where intensity rate increases slightly with C_{N_A} when compared with the trend at the lower Mach numbers.

The root-mean-square values of B_w show that intensity levels for the clean configuration (fig. 7(a)) were considerably higher than for the other configurations, which were all limited to about the same maximum angle of attack.

The similarity of the intensity rise with C_{N_A} for the different configurations and Mach numbers indicates that flow separation in each instance excites the vibratory motion of the wing in a similar manner. Even though the mechanism of flow separation is different for subsonic and transonic Mach numbers (refs. 14 and 15) and the intensity rise is similar, the data suggest that a thin, sharp-edged wing of low aspect ratio is susceptible to severe separation effects with small increases in angle of attack once buffet onset has occurred.

Effect of flaps on buffet intensity. - Figures 8 and 9 present the buffet intensity rise with C_{N_A} for selected leading-edge and trailing-edge flap deflections for Mach numbers of approximately 0.83 and 0.89, respectively. The effects of separate leading- or trailing-edge flap deflection for all configurations tested indicate that significant reductions in the buffet intensity level for given C_{N_A} values can be obtained through deflection of the trailing-edge flap alone (figs. 8(b) and 9(b)). Gains in C_{N_A} of approximately 0.15 for a given intensity level are indicated for maximum deflection of the trailing-edge flap. Increased deflection of the leading-edge flap alone generally produced small gains in C_{N_A} for given intensity levels at a Mach number of approximately 0.83 (fig. 8(a)) but had negligible effect at a Mach number of approximately 0.89 (fig. 9(a)). An average increase in C_{N_A} of approximately 0.07 was obtainable by deflecting the leading-edge flap at a Mach number of approximately 0.83 (fig. 8(a)).

In general, greater values of C_{N_A} could be obtained for any given buffet intensity with the higher wing-flap deflections. The leading-edge flap contribution in reducing the intensity levels ($M \approx 0.83$, fig. 8) is apparently additive to the improvement shown by deflection of the trailing-edge flap alone. For combined flap deflection at a Mach number of approximately 0.89 (fig. 9), however, the leading-edge flap contribution is slight, even though no obvious gains are shown for deflection of the leading-edge flap only.

The clean-wing buffet intensity level at maximum lift for these flight conditions generally did not exceed 6 percent of the maximum steady-state normal acceleration and 8 percent of the maximum steady-state bending moment, as illustrated in figure 3(a).

A similar analysis for the combined flap deflection configurations generally indicated that the intensity levels did not exceed 4 percent of the maximum steady-state normal acceleration and 5 percent of the maximum steady-state bending moment, as illustrated in figure 3(b). For flight conditions where higher dynamic pressures occurred, intensity percentages of the steady-state loads would probably be greater.

Effect of dynamic pressure on buffet loads. - The effects of dynamic pressure on the magnitude of the buffet loads are shown in figure 10 for Mach numbers of approximately 0.69 and 0.85. Results are presented for the clean-wing configuration (figs. 10(a) and 10(c)) and the maximum flap deflection configuration ($\delta_{le} \approx 12°$, $\delta_{te} \approx 13°$) (fig. 10(b)).

As expected, the data for the higher dynamic pressures indicate significant increases in buffet loads for given C_{N_A} levels. The clean-wing intensity levels for the highest dynamic pressure and high lift conditions in some instances are approximately twice the magnitude of the low dynamic pressure data for the same C_{N_A} values. Similar results were obtained at a Mach number of approximately 0.85 for the clean-wing configuration.

Also shown in figure 10 is a difference in C_{N_A} values for buffet onset between the high and low dynamic pressure data. When the buffet-onset level is defined as $\sigma_{a_{n_p}} \approx \pm 0.025g$, the data in some instances indicate a maximum difference in C_{N_A} for buffet onset of approximately 0.1. Reference 5 also shows differences in buffet onset for a similar range of dynamic pressures. Apparently, the vibratory motion of the wing is excited at slightly lower levels of lift at high dynamic pressure conditions.

Frequency Analysis

Estimates of the power-spectral-density distributions of the wing buffet loads and the normal accelerations at the pilot's compartment are presented in figures 11(a) to 11(d). Flight data are shown for low subsonic and transonic Mach numbers for both the clean-wing configuration and the maximum flap deflection configuration ($\delta_{le} \approx 12°$, $\delta_{te} \approx 13°$). The peaks in the data are correlated in the following table with approximate values for the wing natural frequencies as determined by the manufacturer:

Predominant mode	Frequency, Hz
First symmetric wing bending and two-node fuselage vertical bending. (Wing tips in phase with fuselage belly but out of phase with fuselage nose and tail.)	9.66
Second symmetric wing bending and two-node fuselage vertical bending. (Wing tips out of phase with fuselage belly but in phase with fuselage nose and tail.)	13.04
Symmetric wing torsion with node near midchord	36.5

The frequency analysis of figure 11 reveals that most of the power for a_{n_p} occurs between approximately 9 and 22 hertz for all wing configurations and Mach numbers tested. Several peaks are shown in this frequency range, corresponding approximately

to the frequencies listed in the table. The power shown at these frequencies may have been initiated by the natural frequencies of the main structure and may contain additional power arising from local structural vibrations. Some power is also observed at approximately 35 hertz, which correlates with the symmetric wing torsion frequency. Some normal acceleration response may also have occurred at this frequency, although the wing bending sensor showed no response because of its location near a wing torsion node at the midchord of the wing.

The wing structure was found to respond at the second symmetric wing bending mode. No explanation is available of why the wing did not respond at its first bending mode.

Effect of Flaps on Normal Force

The individual and combined effects of leading- or trailing-edge flap deflection on the normal-force curves are shown in figures 12 and 13 for Mach numbers of 0.83 and 0.89, respectively. Buffet intensity levels are superimposed for reference. The level of C_{N_A} for a given angle of attack and leading-edge flap deflection is significantly increased by deflecting the trailing-edge flap. The camber effect due to trailing-edge flap deflection thus causes a significant reduction in the zero-lift angle of attack, as shown in figures 12(b) and 13(b).

For increased deflection of the leading-edge flap only (figs. 12(a) and 13(a)), the data show a slight reduction in C_{N_A} at low angles of attack and the expected increase in C_{N_A} at high angles of attack. The small amount of forward camber added by deflection of the leading-edge flap is highly effective in improving the lift capability at high angles of attack on wings of very low thickness and with sharp leading edges, as typified by the F-104 configuration. The angle-of-attack limitations of the F-104 airplane, however, made it impossible to take full advantage of leading-edge flap deflection. The use of leading-edge flaps on a similar wing configuration is discussed further in reference 14, which shows variations of the wing pressure and load distribution due to increased leading-edge flap deflection at high angles of attack.

Comparisons of the magnitude of lift available from deflection of the leading-edge or trailing-edge flaps in figures 12 and 13 show that, for the angle-of-attack range investigated, significantly greater advantages are realized with the trailing-edge flaps. The results also show, however, that the linearity of the lift curves is limited to a lower angle-of-attack range as trailing-edge flap deflection increases.

The results for combined leading- and trailing-edge flap deflection (figs. 12(c) to 12(e) and figs. 13(c) to 13(e)) indicate that the advantages shown for separate deflection of either the leading- or trailing-edge flap are obtained additively at high angles of attack, with resultant high levels of C_{N_A} at the maximum wing-flap deflections tested.

The superimposed buffet intensity levels in figures 12 and 13 show an increase in available lift for given intensity levels with increased deflection of the trailing-edge flap. In general, the intensity levels at high lift decrease with increasing flap deflection, whether the flaps are deflected individually or in combination.

The normal-force characteristics for the clean wing and for selected wing-flap combinations are presented in figures 14(a) to 14(c) for the range of Mach numbers tested. The results show an increase in C_{N_A} at a given angle of attack with increase in Mach number as well as flap deflection.

Pilot Comments

The pilots reported buffet onset at approximately the same g-level or lift level as indicated by the buffet instrumentation for all configurations tested. Figure 15 is a comparison of the measured buffet boundary for the clean-wing configuration and the buffet onset determined from pilot comments. Agreement of the data is excellent. In general, for most of the test conditions the pilots considered the buffeting to be moderate and not objectionable in maneuvers. At higher levels of dynamic pressure or normal acceleration than tested, the effects of the structural response due to flow separation would probably become objectionable.

The pilots generally agreed that the trailing-edge flap provided a large, worthwhile increase in buffet-free and usable lift beyond the buffet boundary of the clean configuration for all flight conditions tested. They also felt that the leading-edge flap was beneficial in raising the g-level for buffet onset. The increased maneuvering envelope provided by the flaps prior to and after buffet onset was generally appreciated. Also appreciated was the noticeable increase in lift produced by the trailing-edge flap, which resulted in improved turning capability and maneuvering characteristics as compared to the clean-wing configuration. This gain in turning capability with increased flap deflection at elevated lifts was observed at all speeds tested (ref. 8).

As illustrated in figures 16(a) and 16(b), a wing-rock problem characterized by an aperiodic, uncontrollable bank angle oscillation was encountered occasionally. The pilots reported this phenomenon at the higher lift levels over most of the speed range tested, particularly with the larger flap deflections. The wing-rock effects tended to become more severe as lift, angle of attack, and Mach number increased.

CONCLUDING REMARKS

A flight investigation was conducted using an F-104 airplane to assess the effects of wing leading- and trailing-edge flap deflection on buffet characteristics during maneuvering flight.

The buffet boundary for subsonic and transonic Mach numbers was raised appreciably by increasing the flap settings. For all flight conditions of the tests, increased deflection of the trailing-edge flap delayed the buffet onset and buffet intensity rise to a significantly higher airplane normal-force coefficient. Deflection of the leading-edge flap produced some delay in buffet onset and the resulting intensity rise at subsonic speeds, whereas only small benefits were derived at transonic speeds.

Increased deflection of the trailing-edge flap provided appreciable lift increments in the angle-of-attack range covered, whereas the leading-edge flap provided lift

increments only at high angles of attack. Moderate deflection of both the leading- and trailing-edge flaps generally provided more linear lift at high angle of attack and higher lift levels than provided by the clean-wing configuration.

Test maneuvers performed at high dynamic pressure indicated significant increases in the buffet loads for given airplane normal-force coefficients. Frequency analysis revealed that most of the buffet power occurred at the lower modes of vibration of the aircraft structure for the clean and the combined flap configurations.

The pilots appreciated the increased maneuvering envelope provided by the flaps, particularly the improved turn capability. A wing-rock problem was encountered occasionally at high-lift conditions, particularly with the largest flap deflections tested.

Flight Research Center
National Aeronautics and Space Administration
Edwards, Calif., March 31, 1972

REFERENCES

1. Lamar, William E.: Military Aircraft: Technology for the Next Generation - Part Two: Emerging Technologies. Astronaut. Aeron., vol. 7, no. 9, Sept. 1969, pp. 68-78.

2. Ray, Edward J.: Buffet Studies. Langley, Ames, Lewis, and Flight Research Center Support of DOD VFAX/FX Projects: A Progress Report, NASA SP-178, 1968, pp. 15-27.

3. Taylor, Robert T.: Recent Aerodynamic Studies Applicable to High Performance Maneuvering Aircraft. Conference on Aircraft Aerodynamics, NASA SP-124, 1966, pp. 89-103.

4. Ayers, Theodore G.: Application of Supercritical Airfoil to Variable-Wing-Sweep Fighter Airplanes. Langley, Ames, Lewis, and Flight Research Center Support of DOD VFAX/FX Projects: A Progress Report, NASA SP-178, 1968, pp. 29-39.

5. Margolin, Milton; and Chung, Jung G.: F-105F Transonic Buffet Study and Effect of Maneuvering Flaps. Tech. Rep. AFFDL-TR-69-37, Air Force Flight Dynamics Lab., Wright-Patterson Air Force Base, July 1969.

6. Titiriga, A., Jr.: F-5A Transonic Buffet Flight Test. Tech. Rep. AFFDL-TR-69-110, Air Force Flight Dynamics Lab., Wright-Patterson Air Force Base, Dec. 1969.

7. Friend, Edward L.; and Monaghan, Richard C.: Flight Measurements of Buffet Characteristics of the F-111A Variable-Sweep Airplane. NASA TM X-1876, 1969.

8. Fischel, Jack; and Friend, Edward L.: Preliminary Assessment of Effects of Wing Flaps on High Subsonic Flight Buffet Characteristics of Three Airplanes. NASA TM X-2011, 1970.

9. Mechtly, E. A.: The International System of Units - Physical Constants and Conversion Factors. NASA SP-7012, 1969.

10. Richardson, Norman R.; and Pearson, Albin O.: Wind-Tunnel Calibrations of a Combined Pitot-Static Tube, Vane-Type Flow-Direction Transmitter, and Stagnation-Temperature Element at Mach Numbers From 0.60 to 2.87. NASA TN D-122, 1959.

11. Huston, Wilber B.; and Skopinski, T. H.: Probability and Frequency Characteristics of Some Flight Buffet Loads. NACA TN 3733, 1956.

12. Bendat, Julius S.; and Piersol, Allan G.: Measurement and Analysis of Random Data. John Wiley & Sons, Inc., 1967.

13. Baker, Thomas F.; Martin, James A.; and Scott, Betty J.: Flight Data Pertinent to Buffeting and Maximum Normal-Force Coefficient of the Douglas X-3 Research Airplane. NACA RM H57H09, 1957.

14. Keener, Earl R. ; McLeod, Norman J. ; and Taillon, Norman V. : Effect of Leading-Edge-Flap Deflection on the Wing Loads, Load Distributions, and Flap Hinge Moments of the Douglas X-3 Research Airplane at Transonic Speeds. NACA RM H58D29, 1958.

15. Pearcey, H. H. : Shock-Induced Separation and its Prevention by Design and Boundary Layer Control. Vol. 2 of Boundary Layer and Flow Control, part IV, G. V. Lachmann, ed., Pergamon Press, 1961, pp. 1166-1344.

TABLE 1. – PHYSICAL CHARACTERISTICS OF THE F-104 AIRPLANE

Wing -	
Area, m^2 (ft^2)	18.2 (196.1)
Span, m (ft)	6.68 (21.9)
Mean aerodynamic chord, m (ft)	2.91 (9.55)
Aspect ratio	2.45
Taper ratio	0.378
Sweepback of 25-percent chord, deg	18.1
Dihedral, deg	-10
Incidence, deg	0
Geometric twist, deg	0
Root chord, m (ft)	3.96 (12.99)
Tip chord, m (ft)	1.49 (4.89)
Section	Modified biconvex
Thickness ratio	0.0336
Straight element, percent chord	70
Location of 25-percent mean aerodynamic chord, fuselage station, m (in.)	12.00 (472.51)
Leading-edge flap (per side) -	
Type	Plain
Area, m^2 (ft^2)	0.79 (8.5)
Chord, percent wing chord	10.6
Spanwise location, percent semispan:	
Inboard end	30.5
Outboard end	94.3
Trailing-edge flap (per side) -	
Type	Plain
Area, m^2 (ft^2)	1.07 (11.55)
Chord, percent wing chord	26.4
Spanwise location, percent semispan:	
Inboard end	27.4
Outboard end	69.2
Ailerons -	
Type	Plain flap
Area, total, m^2 (ft^2)	0.88 (9.46)
Aileron travel, deg:	
Gear extended	±20
Gear retracted	±9.5
Trim travel, deg	±5
Horizontal tail -	
Area, m^2 (ft^2)	4.48 (48.2)
Span, m (ft)	3.63 (11.9)
Mean aerodynamic chord, m (ft)	1.34 (4.41)
Aspect ratio	2.95
Taper ratio	0.311

TABLE 1. – Concluded.

Sweepback of 25-percent chord, deg	10.1
Section	Modified biconvex
Thickness ratio:	
Root	0.0493
Tip	0.0261
Root chord, m (ft)	1.88 (6.16)
Tip chord, m (ft)	0.59 (1.92)
Location of 25-percent mean aerodynamic chord, fuselage station, m (ft)	17.70 (58.08)
Deflection range, deg	5 to -17
Trim level, deg	2 to -11
Vertical tail -	
Area, m^2 (ft^2)	4.06 (43.7)
Mean aerodynamic chord, m (ft)	2.70 (8.88)
Sweepback of 25-percent chord, deg	32.2
Section	Modified biconvex
Location of 25-percent mean aerodynamic chord, fuselage station, m (in.)	16.75 (659.3)
Rudder -	
Type	Plain flap
Area, m^2 (ft^2)	0.51 (5.5)
Deflection range, deg:	
Gear extended	±20
Gear retracted	±6
Trim travel, deg	±4
Ventral fin -	
Area, m^2 (ft^2)	0.54 (5.78)
Length, m (ft)	2.37 (7.79)
Depth, maximum, m (ft)	0.40 (1.31)
Thickness ratio, percent	2.5
Fuselage -	
Frontal area, projected except for swept-up aft section, m^2 (ft^2)	2.32 (25.0)
Length, m (ft)	15.62 (51.25)
Fineness ratio	9.09

TABLE 2. – AIRPLANE WING CONFIGURATIONS TESTED
[Nominal conditions]

Wing-flap position, deg		M	q, N/m^2 (lb/ft^2)
δ_{le}	δ_{te}		
0	0	0.67 to 0.94	13,400 (280)
4	11	.72 to .94	↓
12	13	.67 to .92	
3	0	0.83 and 0.89	13,400 (280)
7	0	↓	↓
10	0		
0	5		
0	10		
0	13		
3	5		
3	10		
3	13		
7	5		
7	10		
7	13		
11	4		
11	10		
11	12		
0	0	0.69	9,100 (190)
0	0	↓	13,400 (280)
0	0		23,000 (480)
12	13		9,100 (190)
12	13		13,400 (280)
12	13		19,200 (400)
0	0	0.85	9,600 (200)
0	0	↓	14,400 (300)
0	0		24,000 (500)

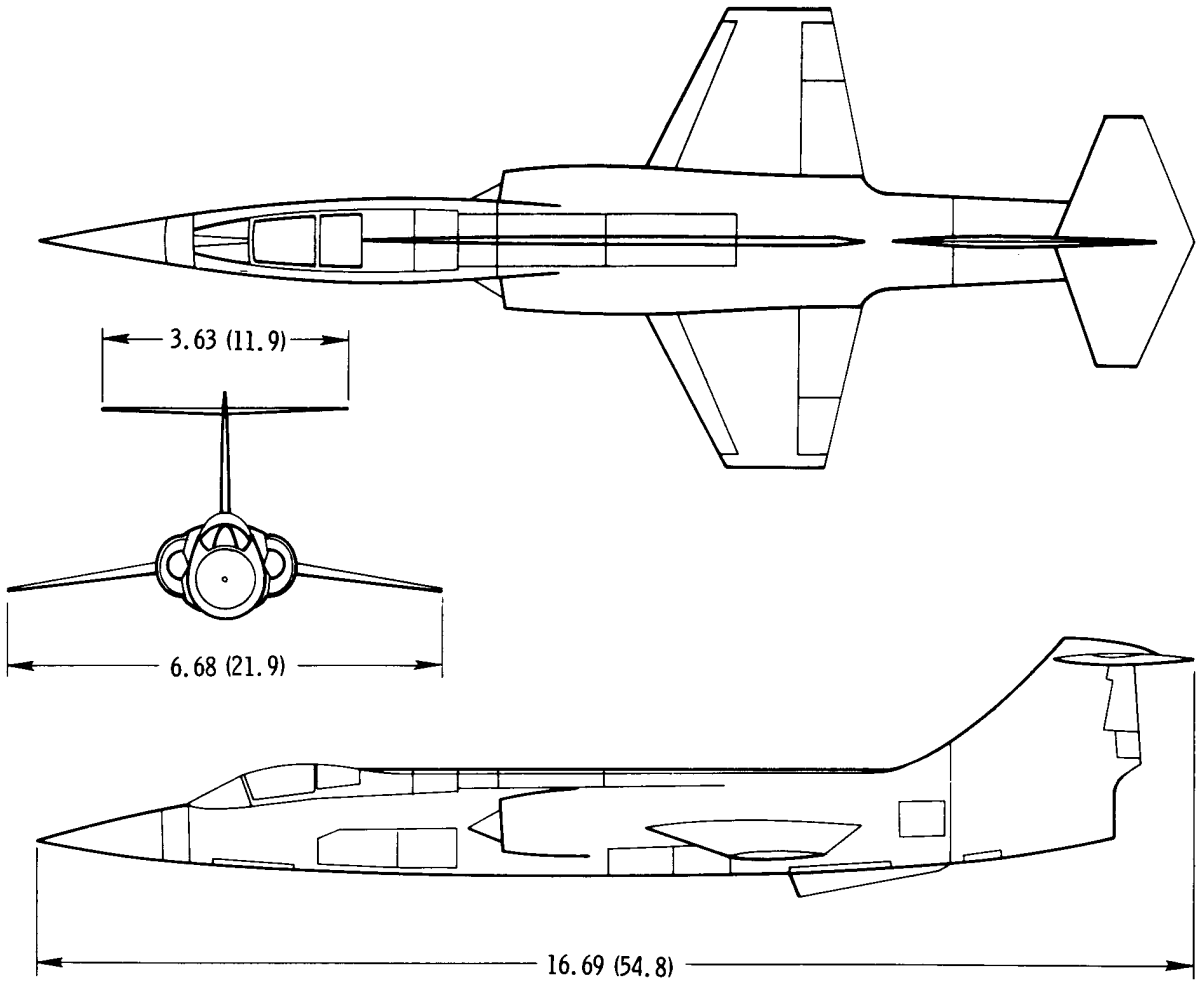

Figure 1. Three-view drawing of the F-104 test airplane. Dimensions in meters (feet).

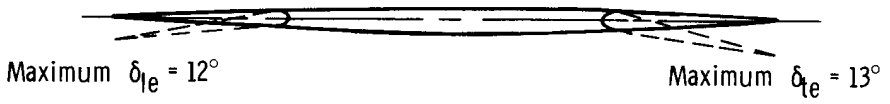

(a) Typical airfoil section.

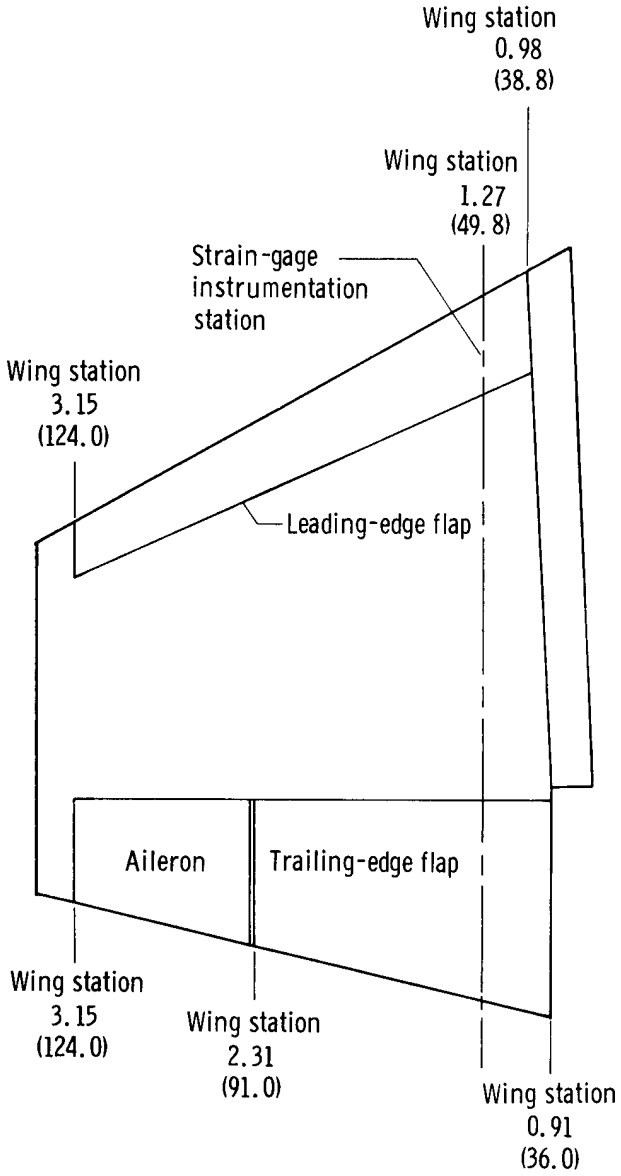

(b) Plan view.

Figure 2. F-104 wing panel. Dimensions in meters (inches).

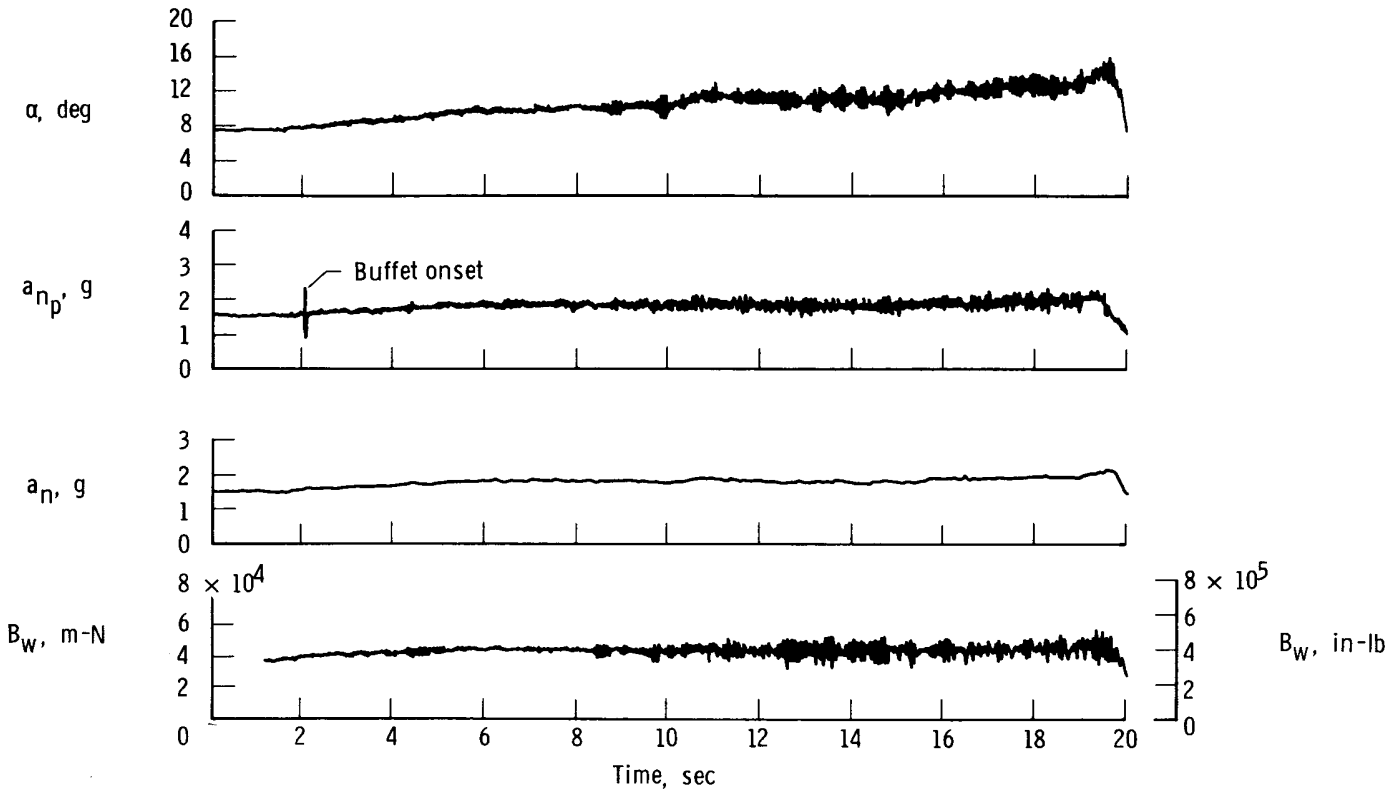

(a) Clean configuration

Figure 3. Typical time history of a windup turn showing strain-gage and flight parameters during buffeting.

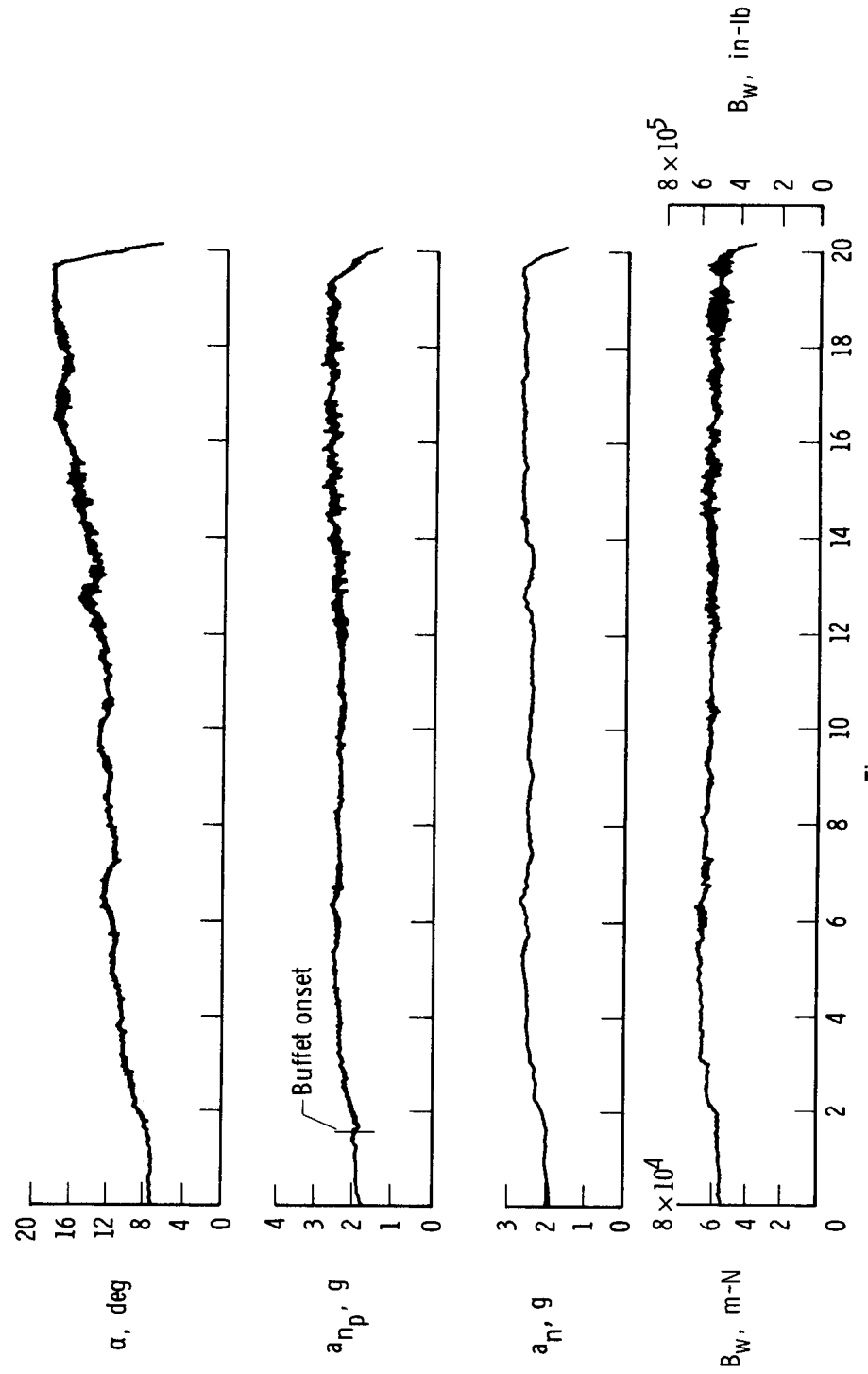

(b) $\delta_{le} = 12°$, $\delta_{te} = 13°$.

Figure 3. Concluded.

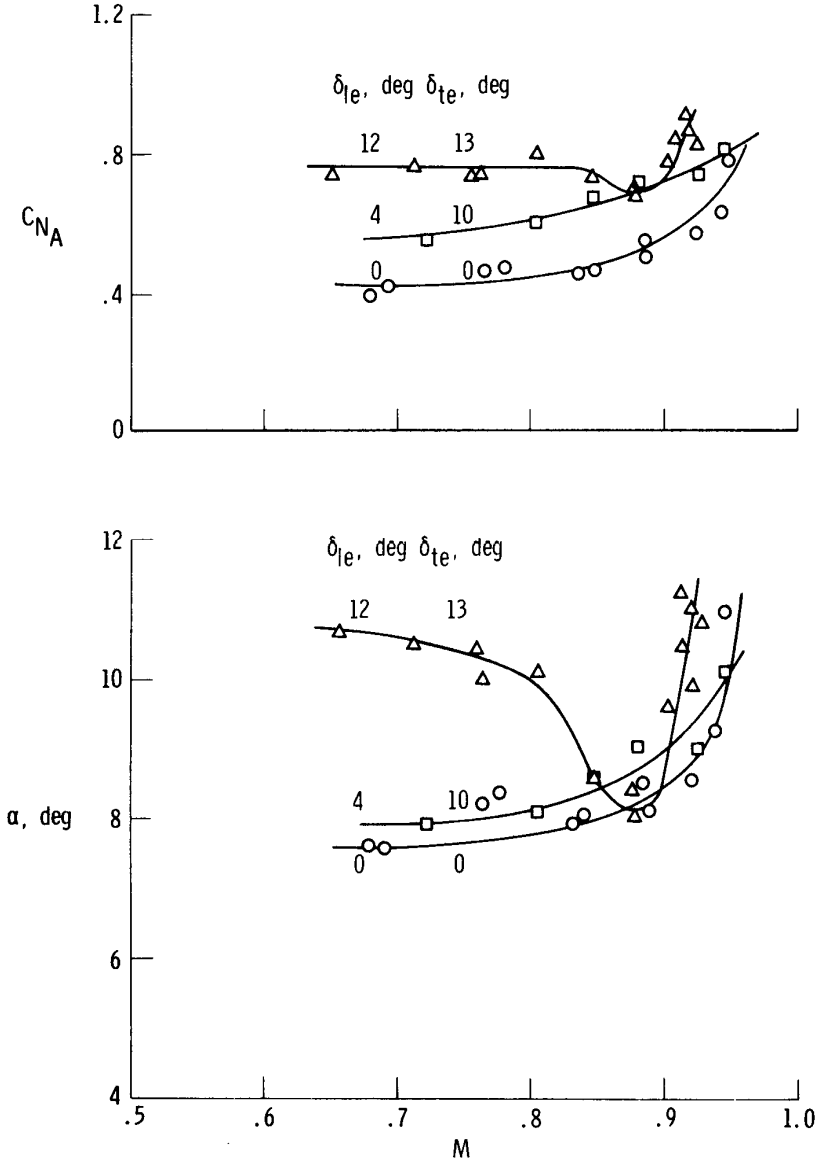

Figure 4. Effect of leading- and trailing-edge flap deflection on the variation with Mach number of airplane normal-force coefficient and angle of attack for buffet onset.

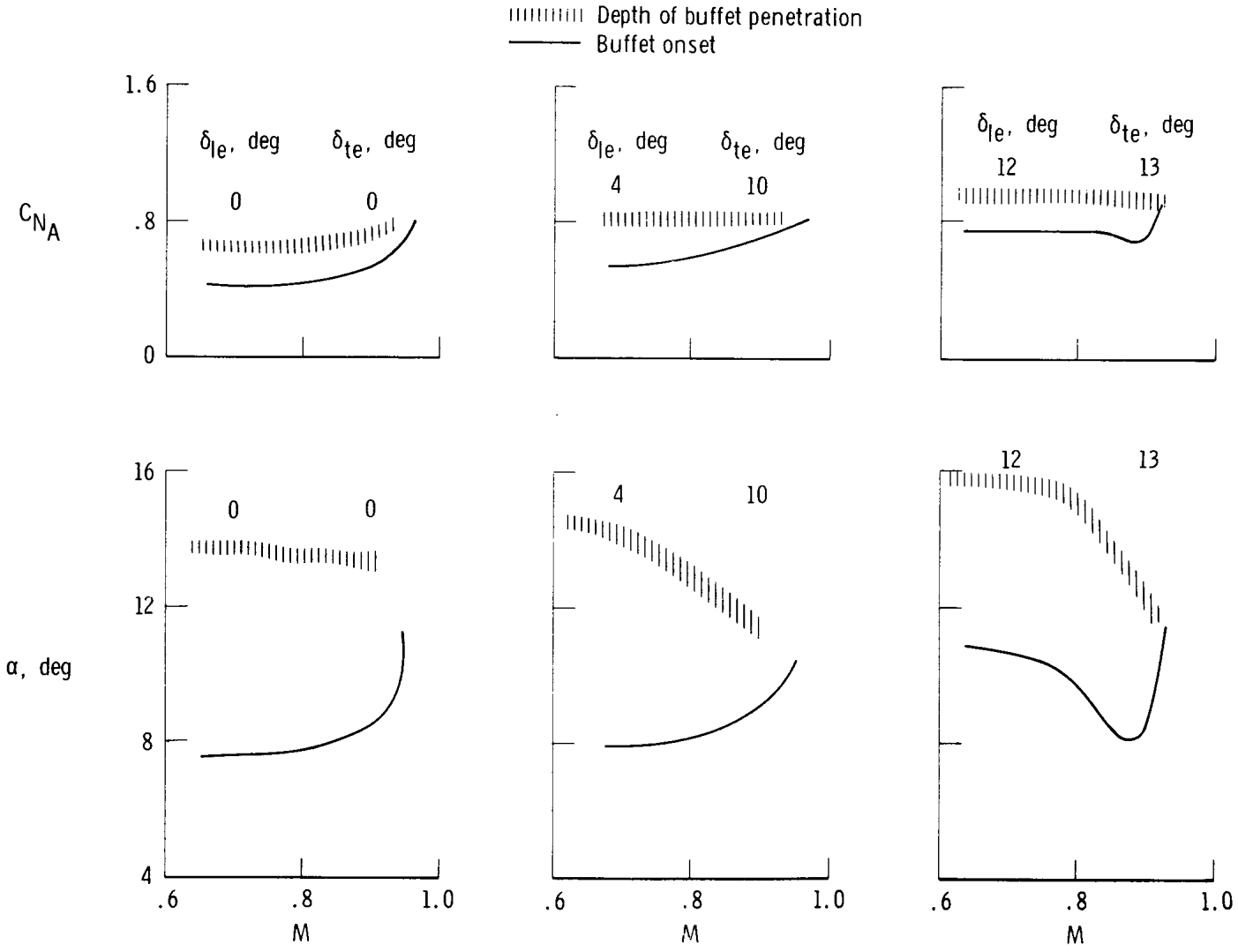

Figure 5. Depth of buffet penetration in relation to buffet-onset boundaries.

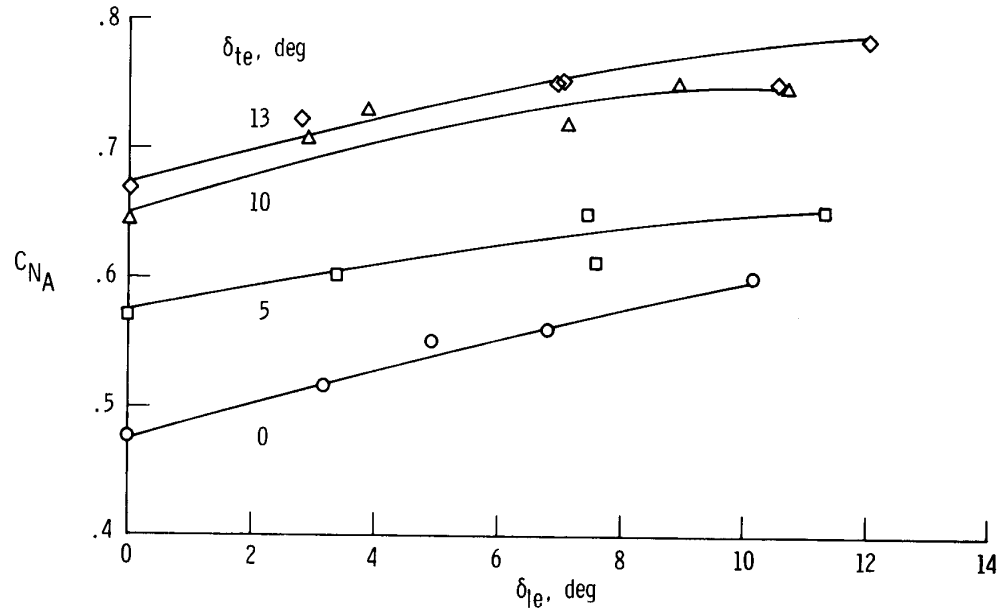

(a) $M \approx 0.83$.

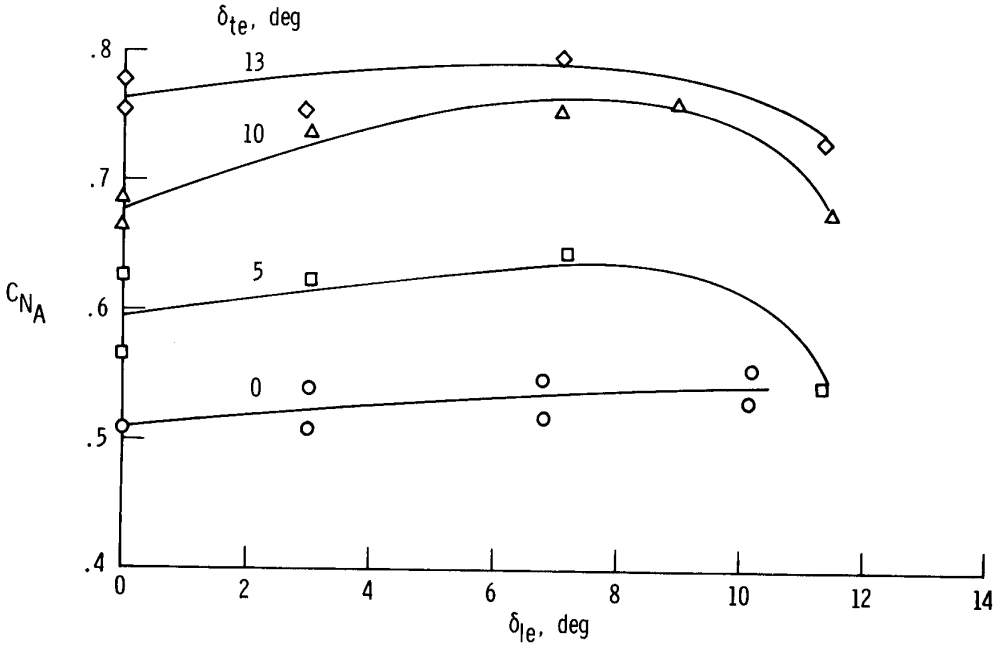

(b) $M \approx 0.89$.

Figure 6. Variation of airplane normal-force coefficient for buffet onset with deflection of wing leading- and trailing-edge flaps.

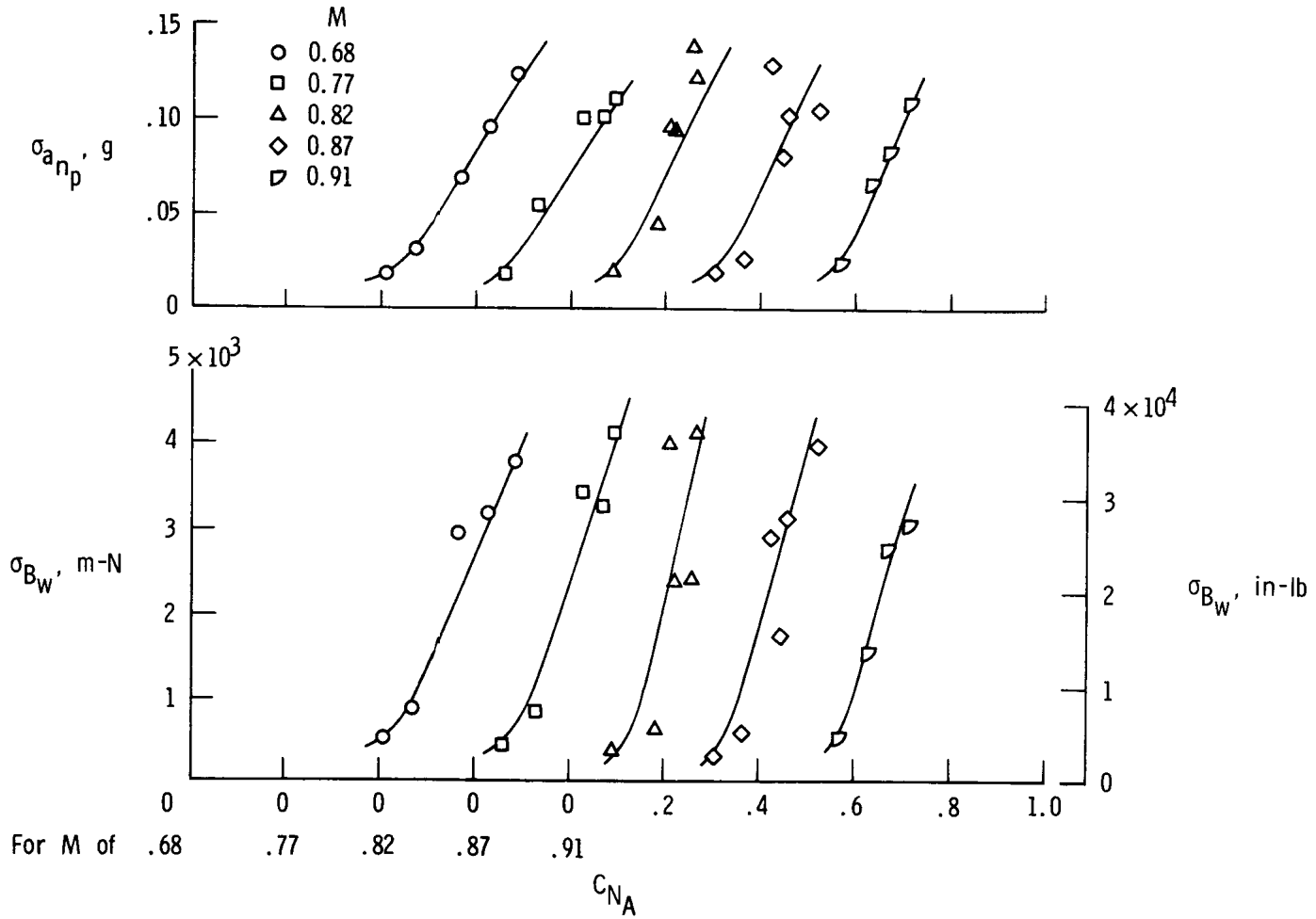

(a) Clean configuration.

Figure 7. Buffet loads at selected Mach numbers. $q \approx 13,400$ N/m^2 (280 lb/ft^2).

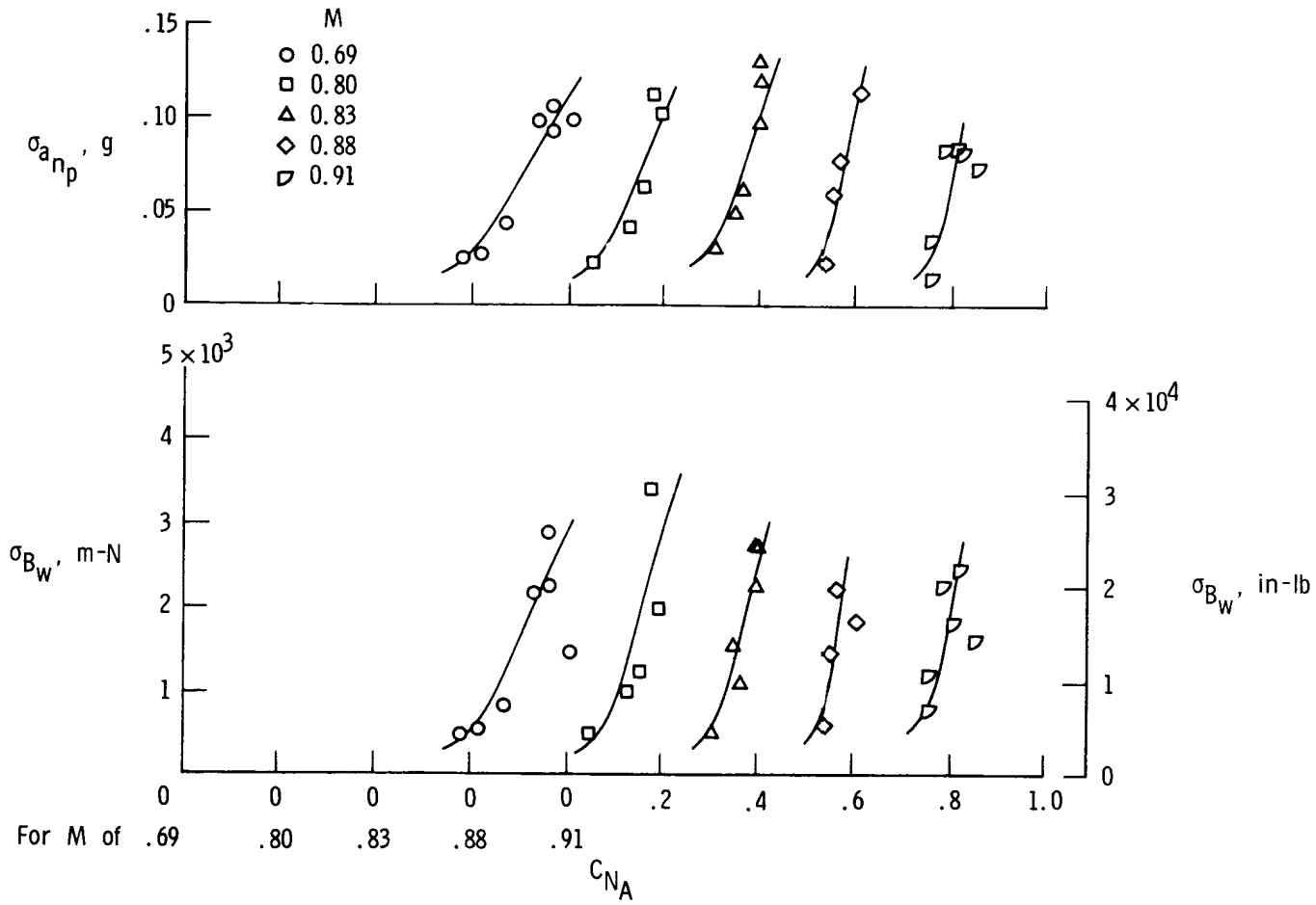

(b) $\delta_{le} = 4°$, $\delta_{te} = 10°$.

Figure 7. Continued.

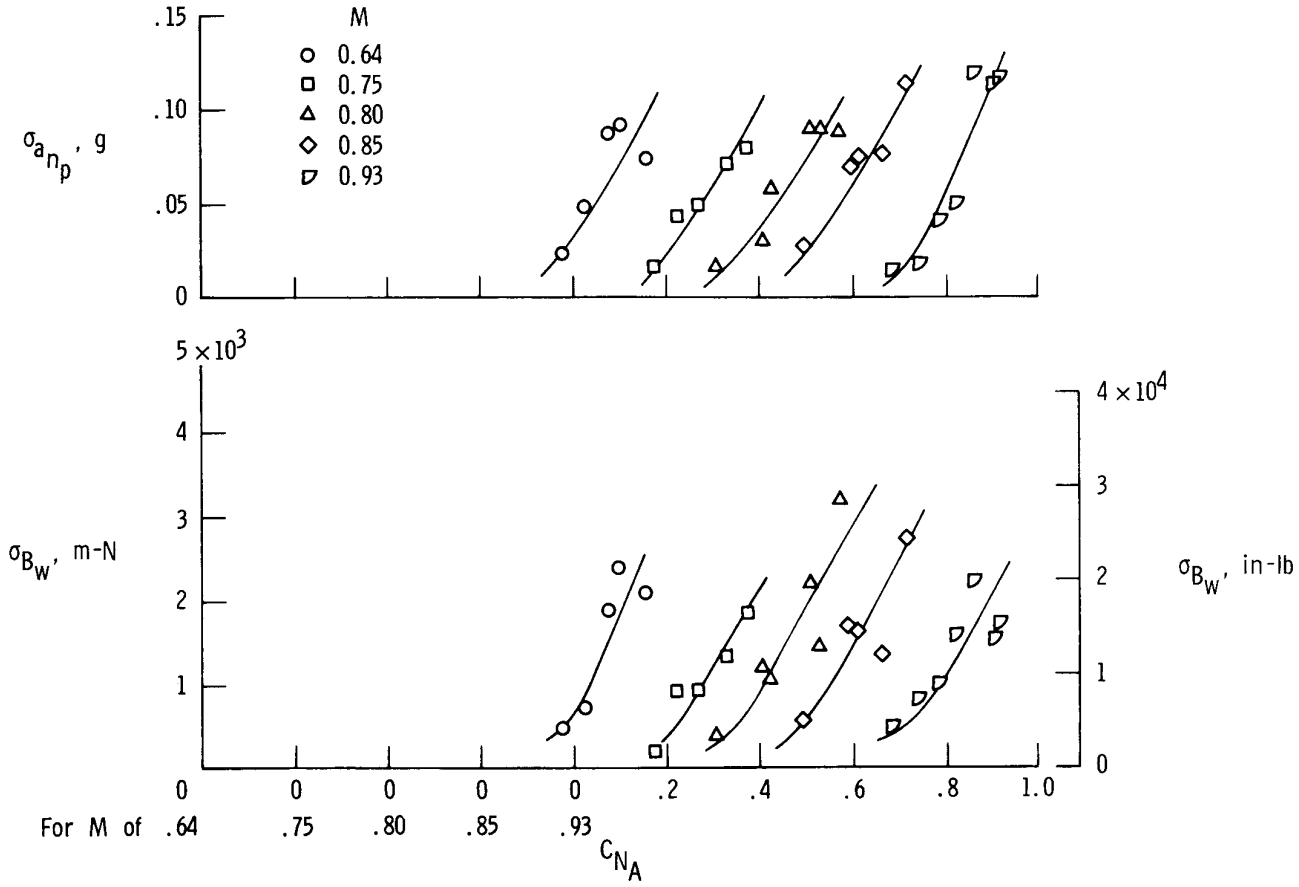

(c) $\delta_{le} = 12°$, $\delta_{te} = 13°$.

Figure 7. Concluded.

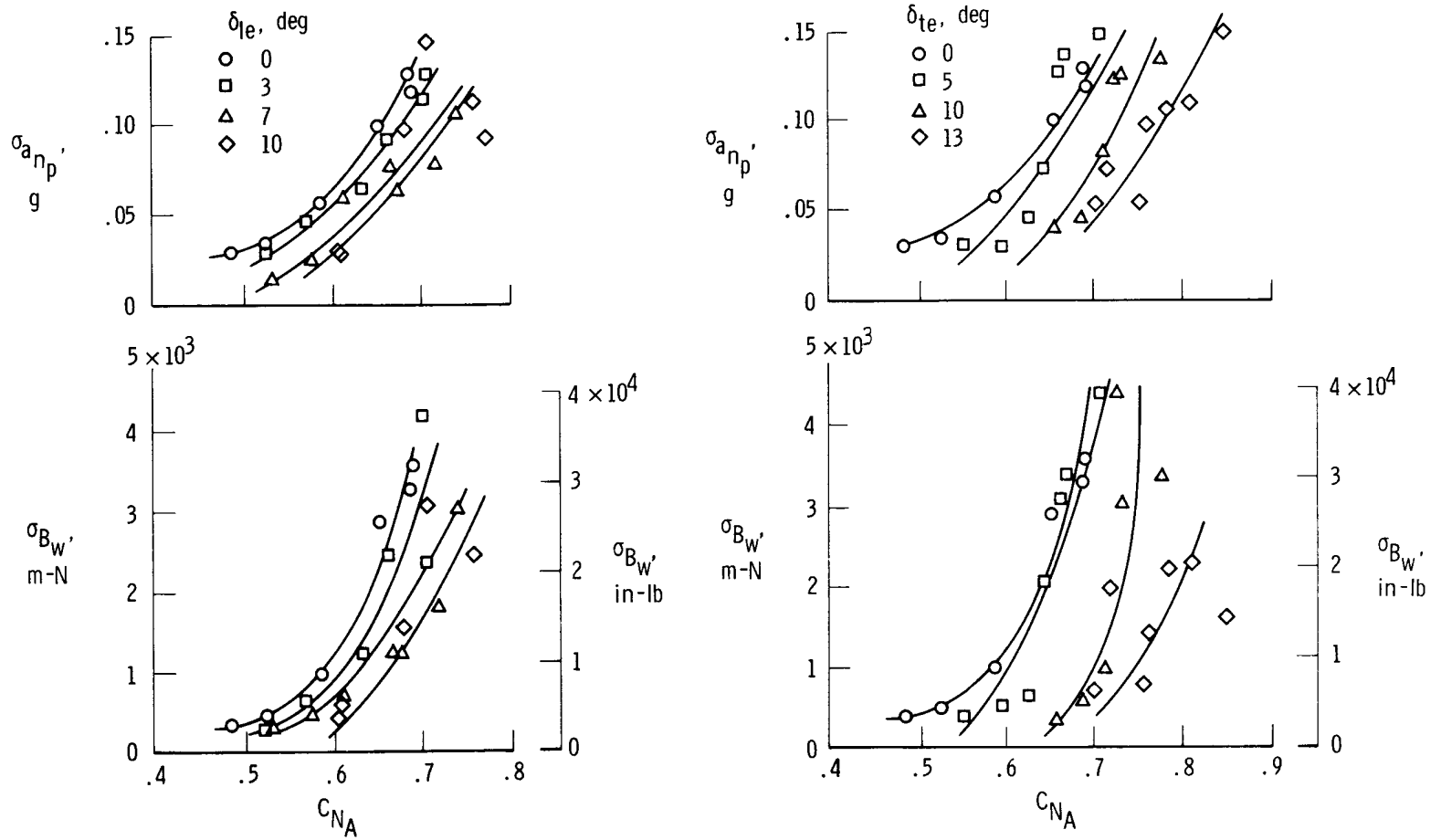

(a) Selected δ_{le} positions, $\delta_{te} = 0°$.

(b) $\delta_{le} = 0°$, selected δ_{te} positions.

Figure 8. Variation of buffet intensity with airplane normal-force coefficient for selected wing-flap deflections at $M \approx 0.83$. $q \approx 13,400$ N/m^2 (280 lb/ft^2).

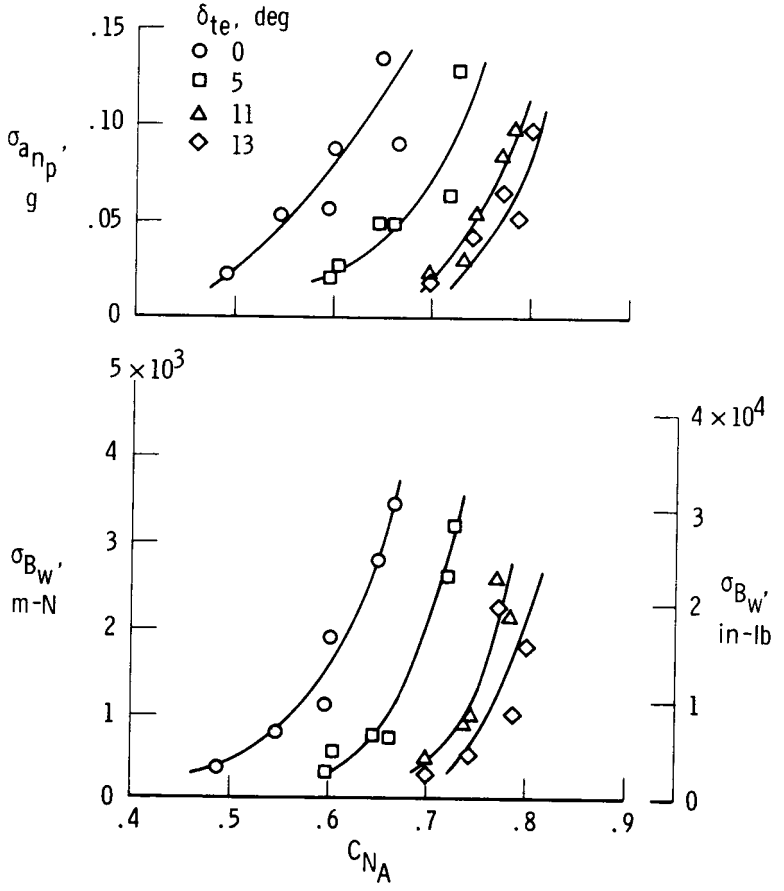

(c) $\delta_{le} = 3°$, selected δ_{te} positions.

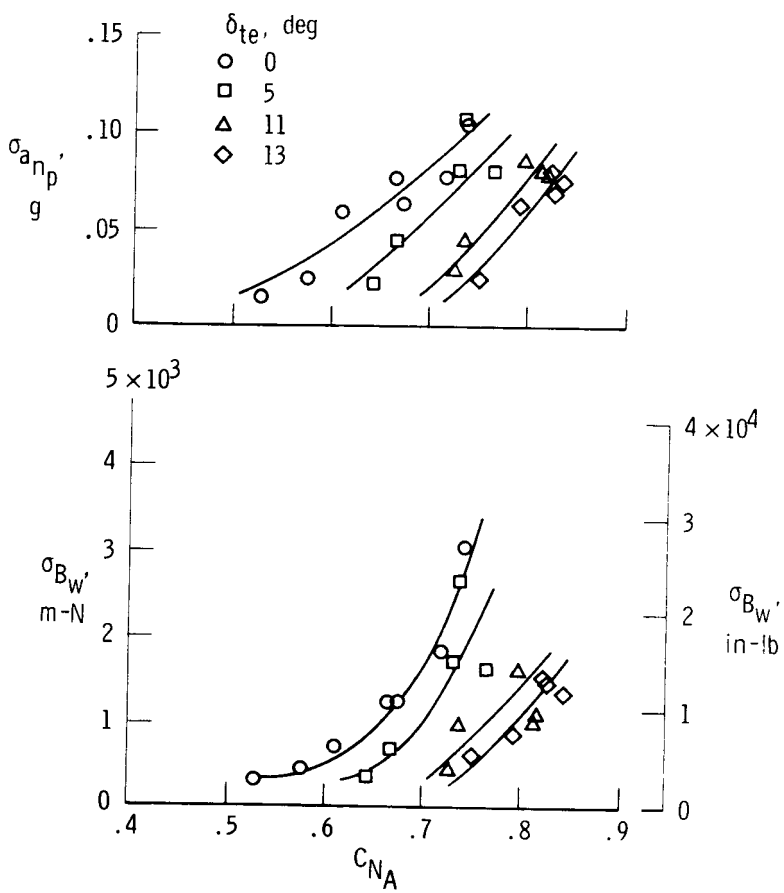

(d) $\delta_{le} = 7°$, selected δ_{te} positions.

Figure 8. Continued.

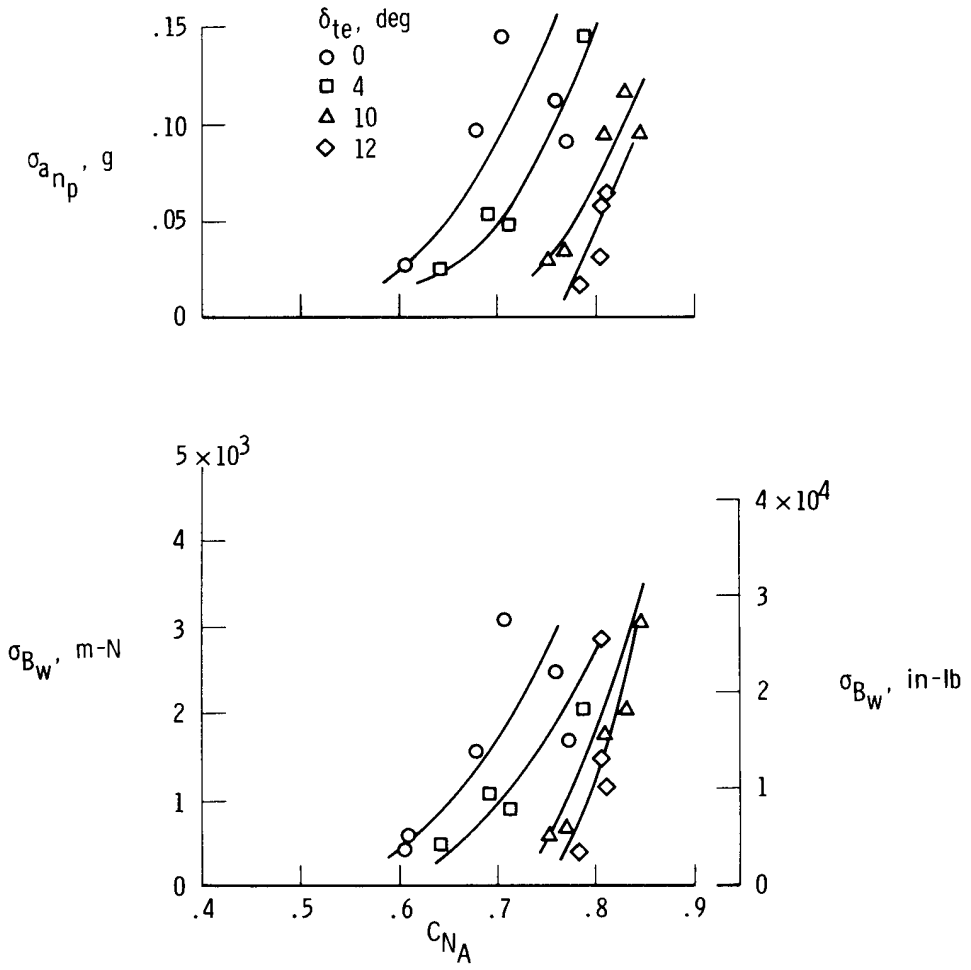

(e) $\delta_{le} = 11°$, selected δ_{te} positions.

Figure 8. Concluded.

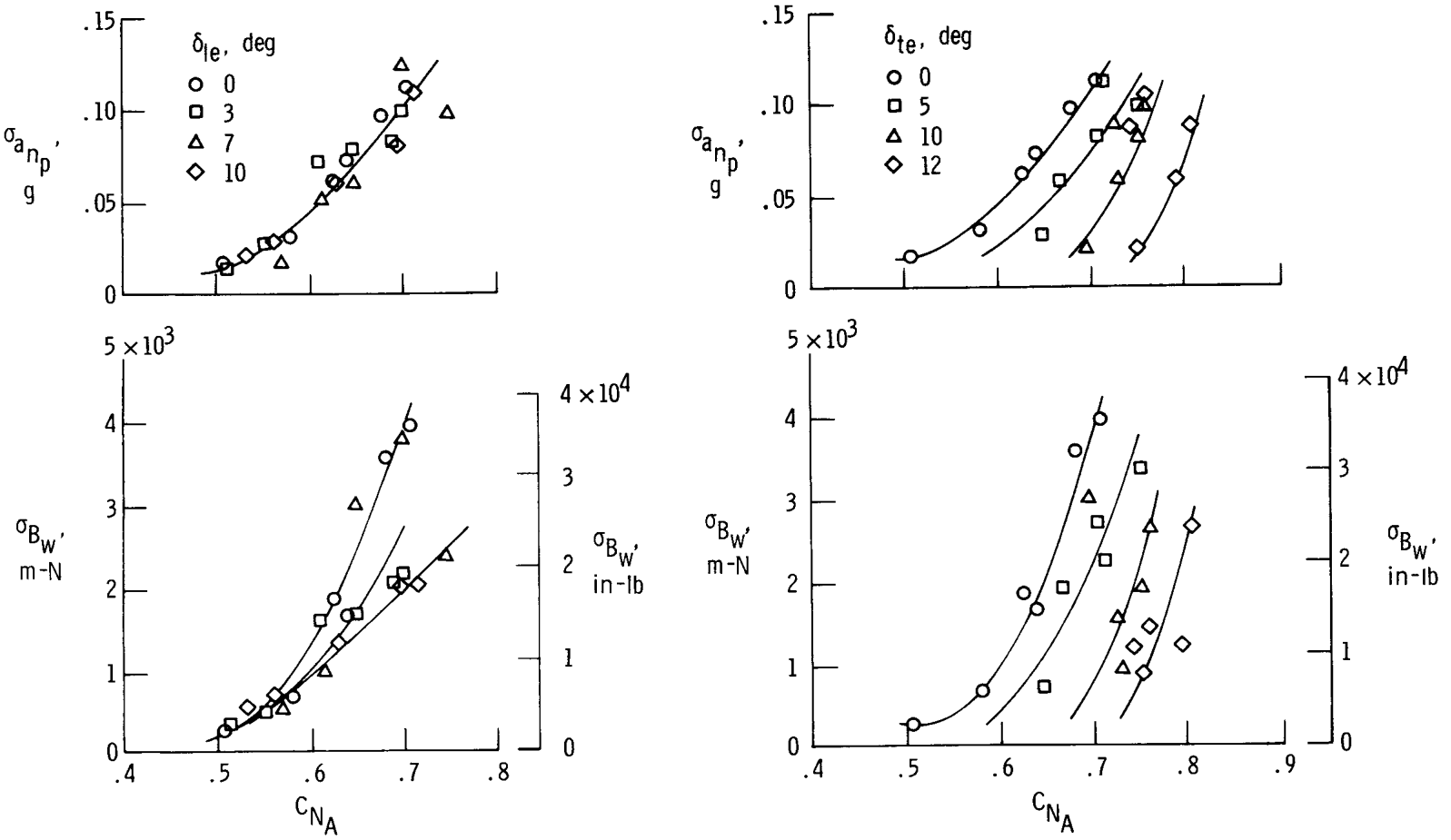

(a) Selected δ_{le} positions, $\delta_{te} = 0°$.

(b) $\delta_{le} = 0°$, selected δ_{te} positions.

Figure 9. Variation of buffet intensity with airplane normal-force coefficient for selected wing-flap deflections at $M \approx 0.89$. $q \approx 13,400$ N/m^2 (280 lb/ft^2).

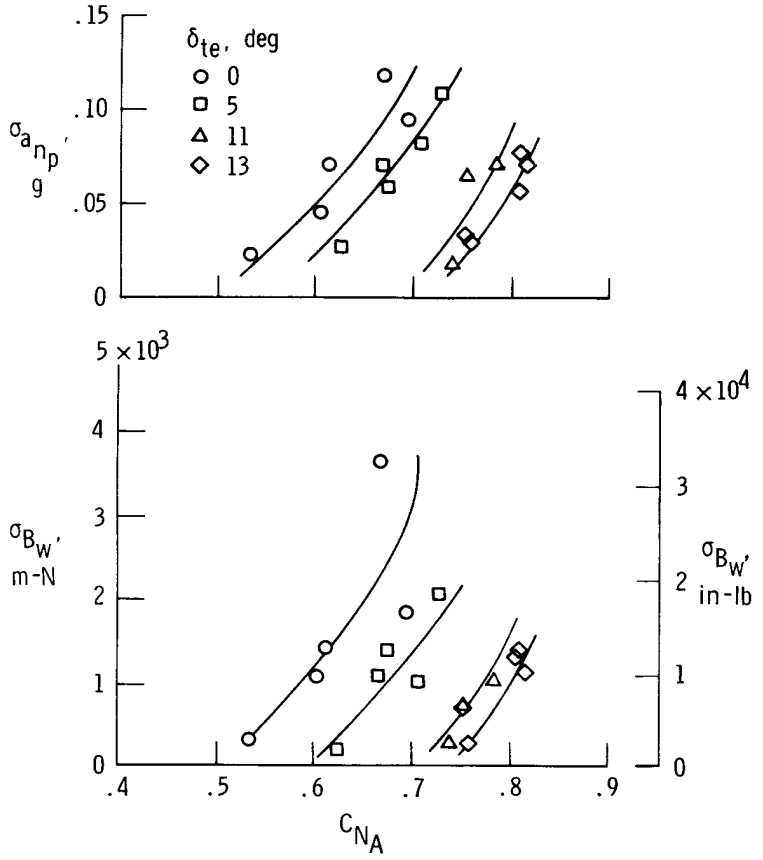

(c) $\delta_{le} = 3°$, selected δ_{te} positions.

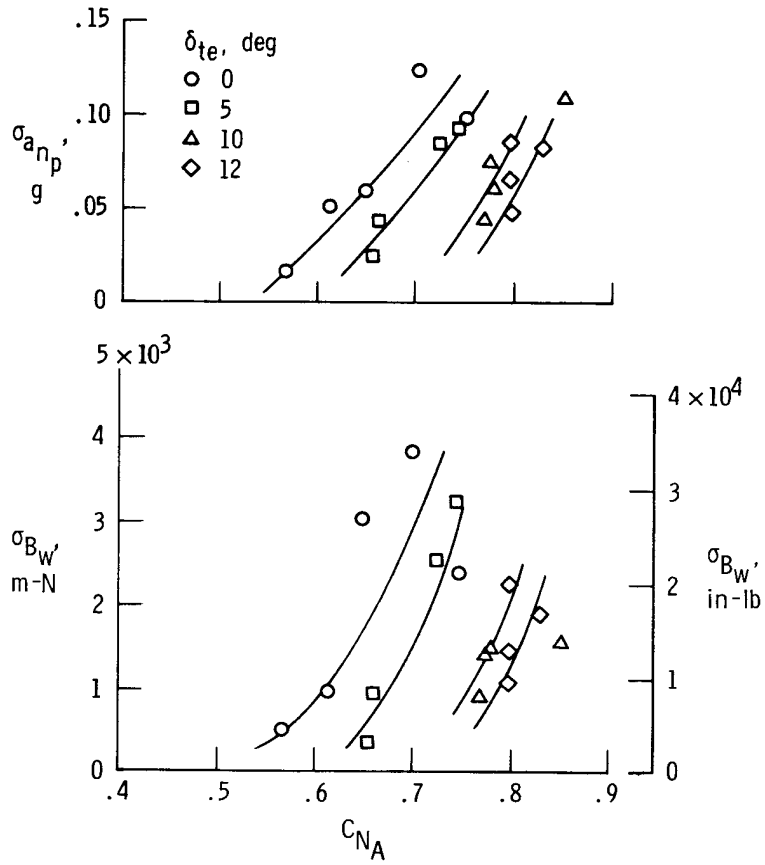

(d) $\delta_{le} = 7°$, selected δ_{te} positions.

Figure 9. Continued.

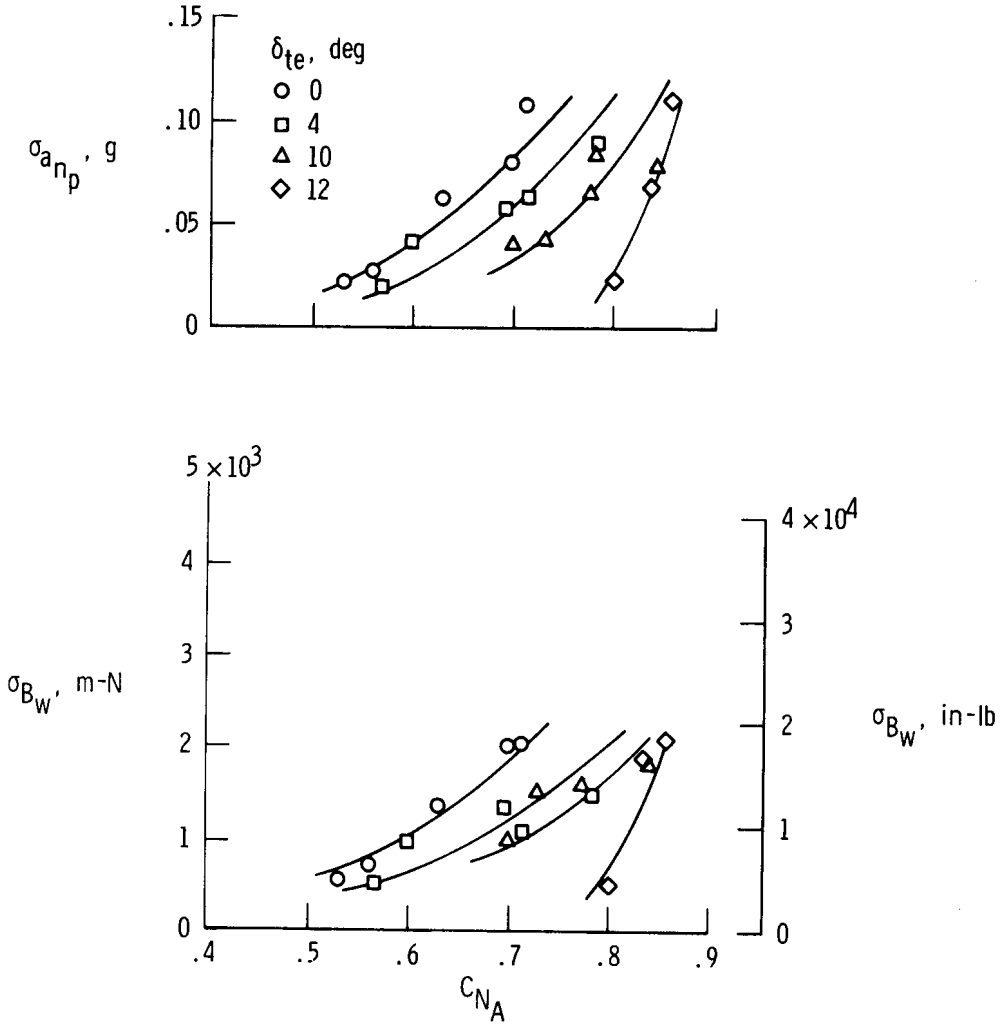

(e) $\delta_{le} = 11°$, selected δ_{te} positions.

Figure 9. Concluded.

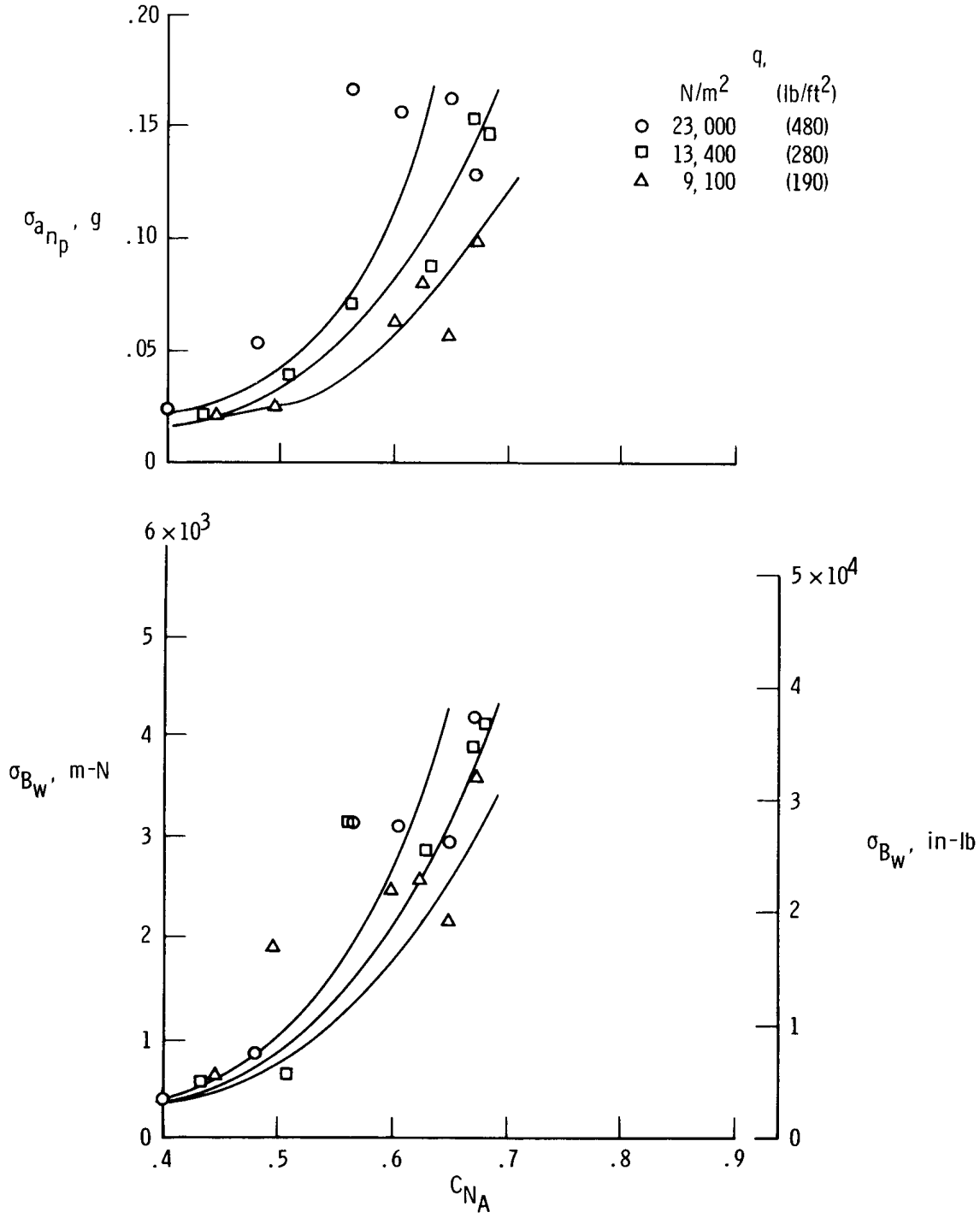

(a) Clean configuration, M ≈ 0.69.

Figure 10. Buffet intensity as a variation of dynamic pressure.

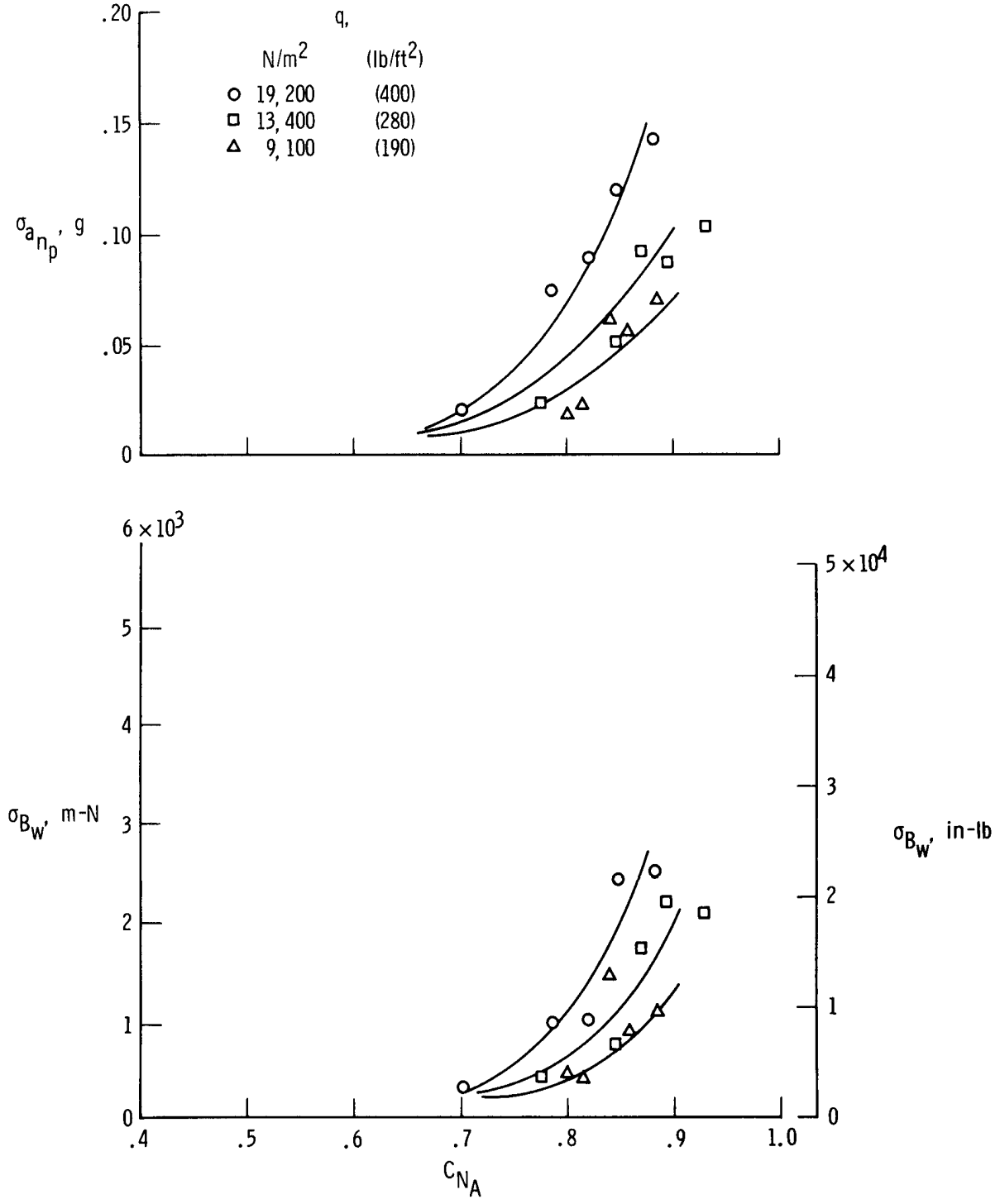

(b) $\delta_{le} = 12°$, $\delta_{te} = 13°$, $M \approx 0.69$.

Figure 10. Continued.

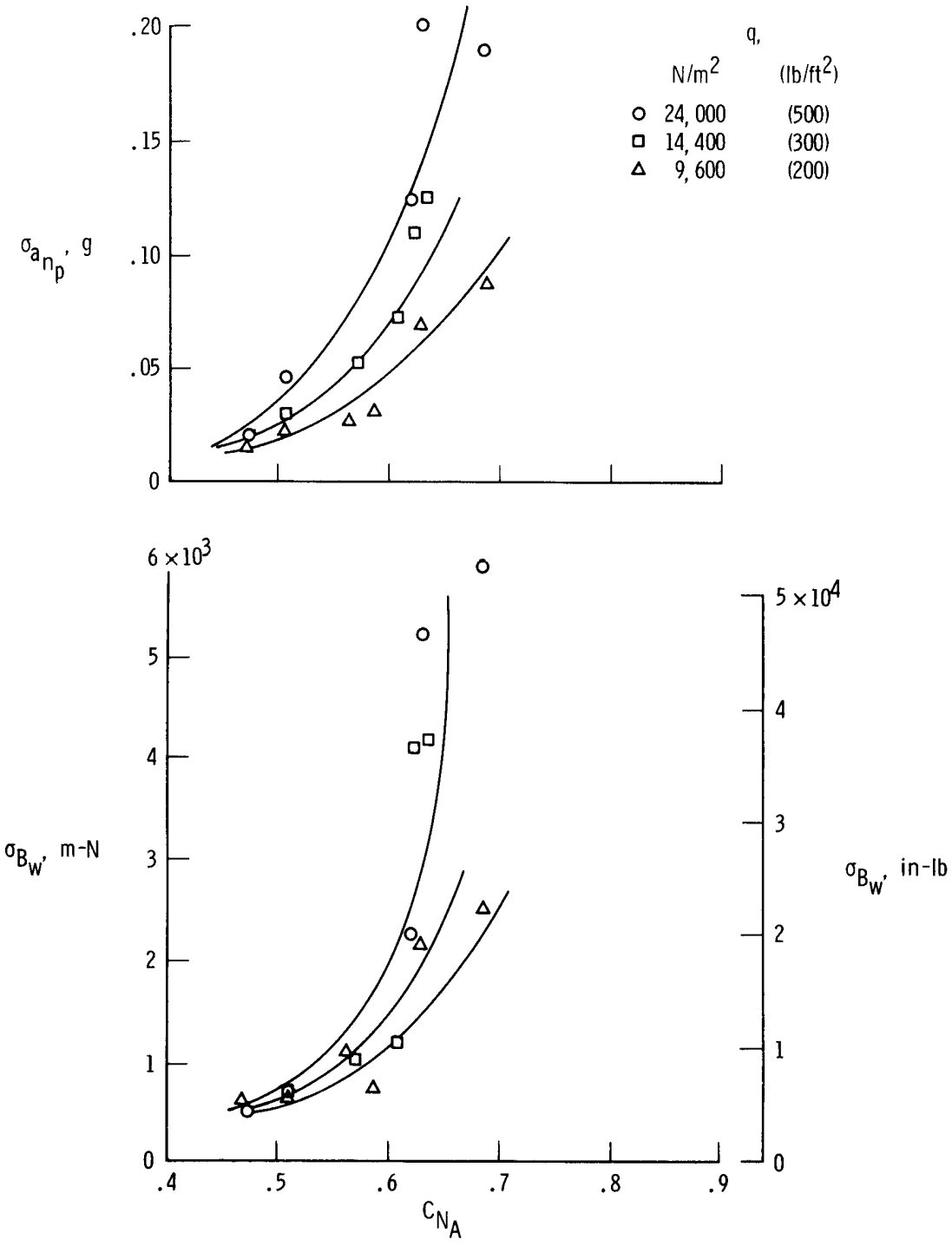

(c) Clean configuration, M $\approx$ 0.85.

Figure 10. Concluded.

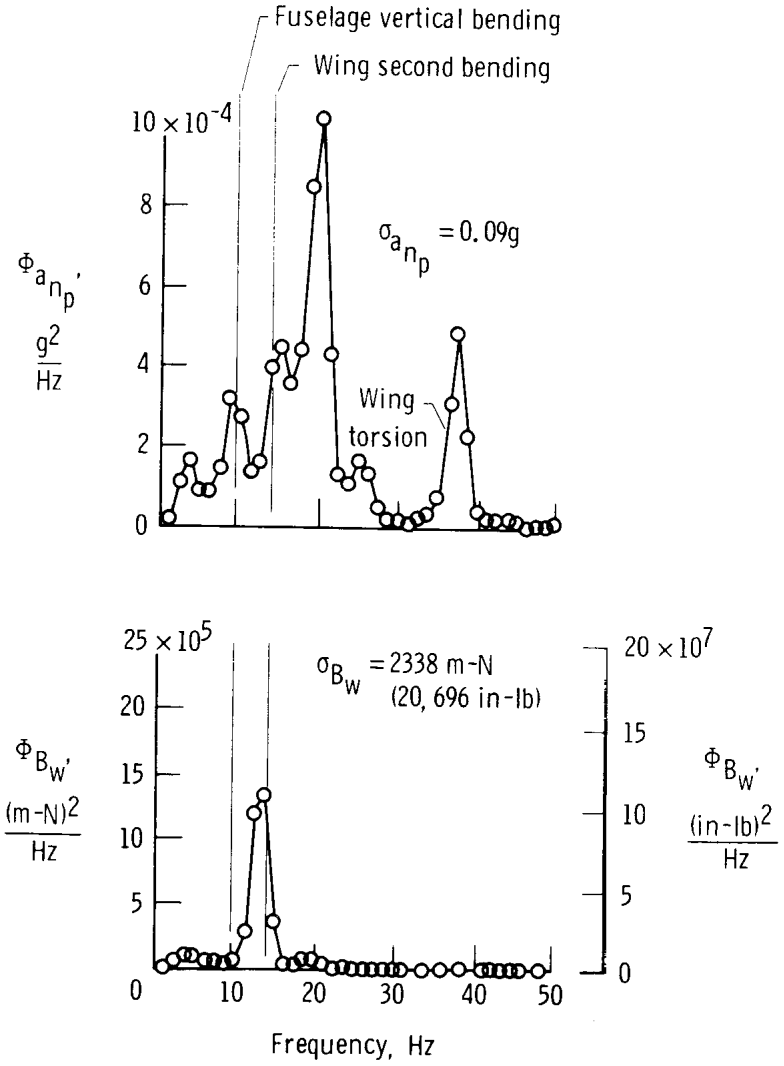

(a) $M \approx 0.69$, $q \approx 13,400$ N/m^2 (280 lb/ft^2), $C_{N_A} = 0.58$, $\alpha = 10.8°$, $\delta_{le} = 0°$, $\delta_{te} = 0°$.

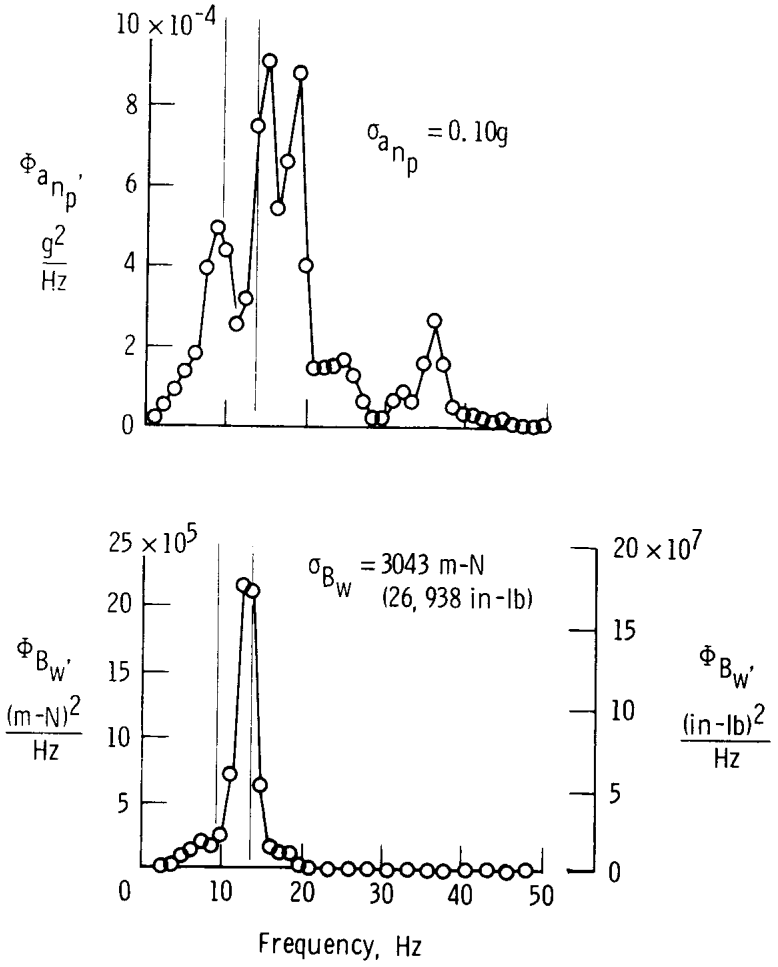

(b) $M \approx 0.67$, $q \approx 13,000$ N/m^2 (270 lb/ft^2), $C_{N_A} = 0.92$, $\alpha = 14.5°$, $\delta_{le} = 12°$, $\delta_{te} = 13°$.

Figure 11. Frequency analysis.

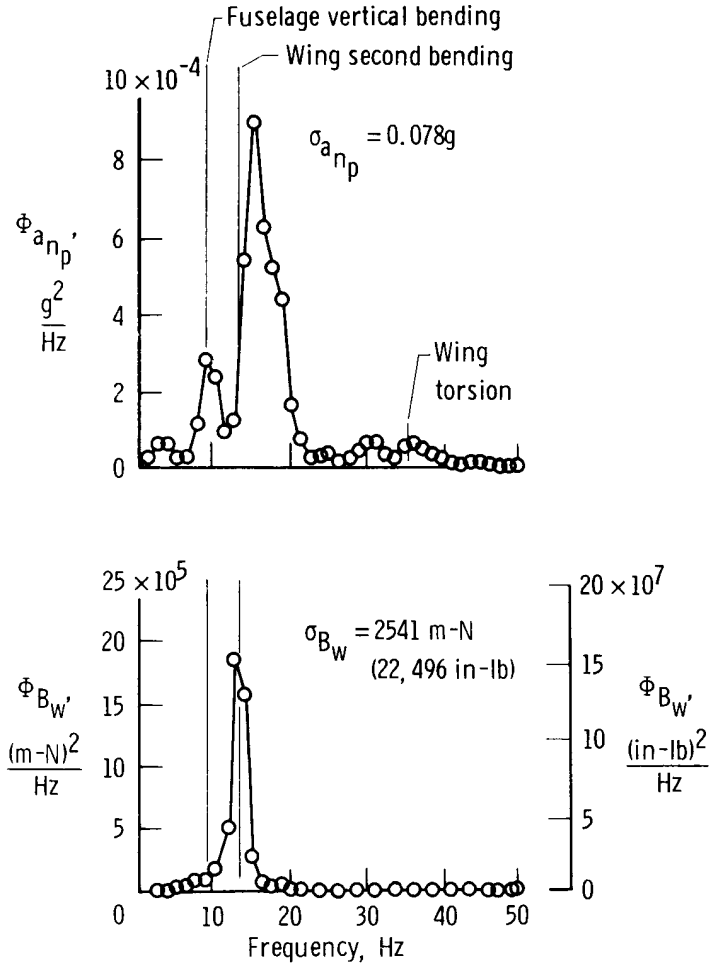

(c) $M \approx 0.83$, $q \approx 13{,}000$ N/m^2 (270 lb/ft^2), $C_{N_A} = 0.94$, $\alpha = 15°$, $\delta_{le} = 12°$, $\delta_{te} = 13°$.

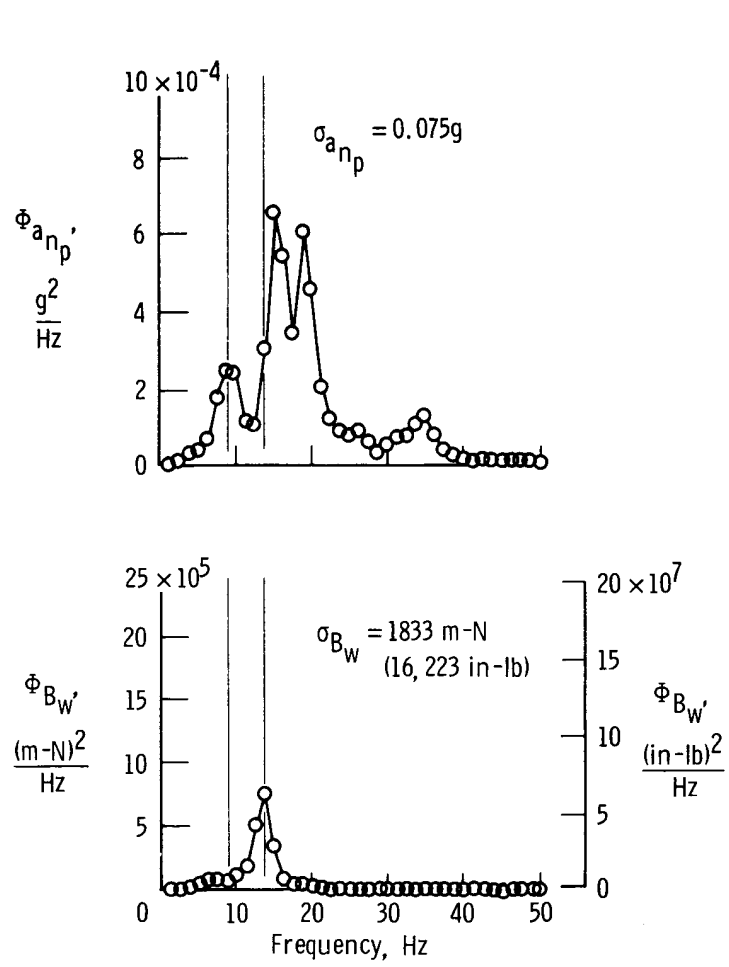

(d) $M \approx 0.86$, $q \approx 13{,}000$ N/m^2 (270 lb/ft^2), $C_{N_A} = 0.66$, $\alpha = 12°$, $\delta_{le} = 0°$, $\delta_{te} = 0°$.

Figure 11. Concluded.

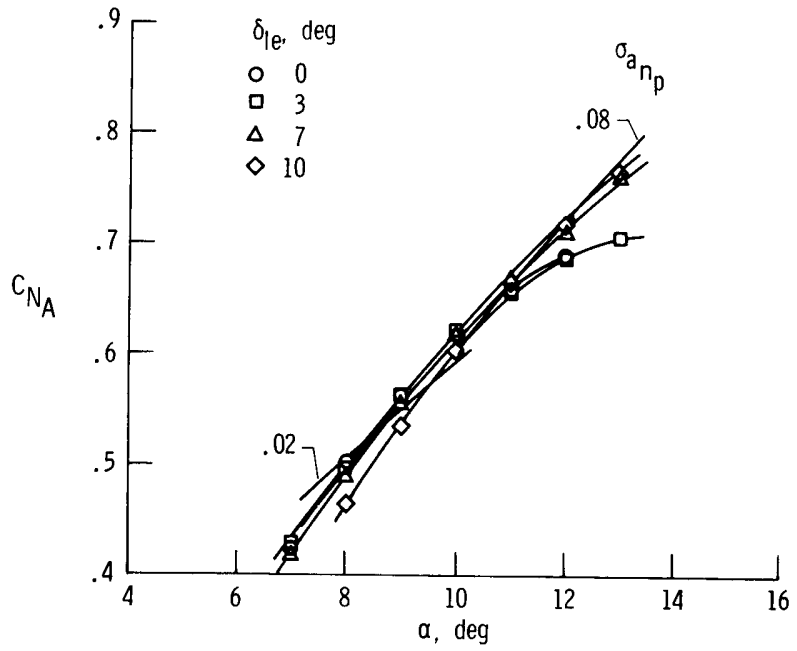

(a) Selected δ_{le} positions, $\delta_{te} = 0°$.

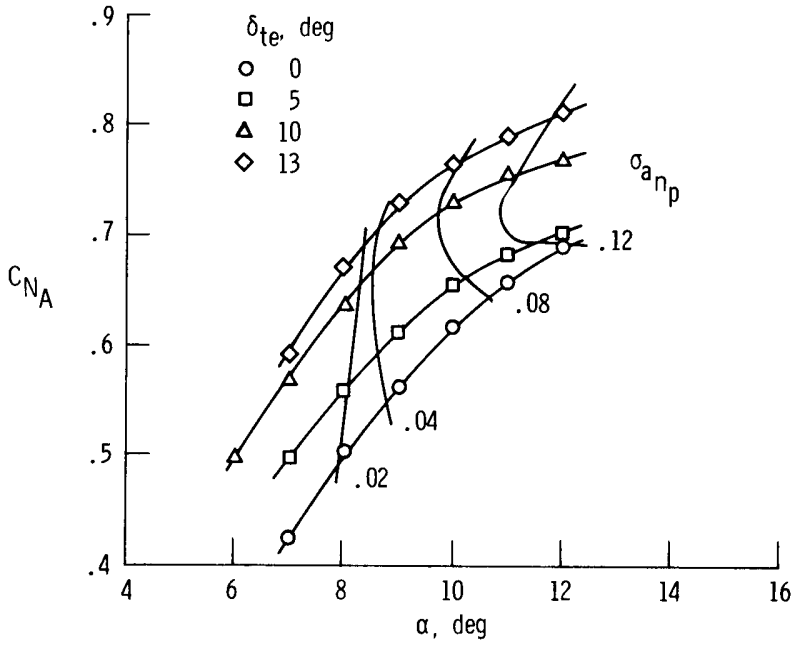

(b) $\delta_{le} = 0°$, selected δ_{te} positions.

Figure 12. Effect of wing-flap deflection on the variation of airplane normal-force coefficient with angle of attack at $M \approx 0.83$. $q \approx 13,400$ N/m^2 (280 lb/ft^2).

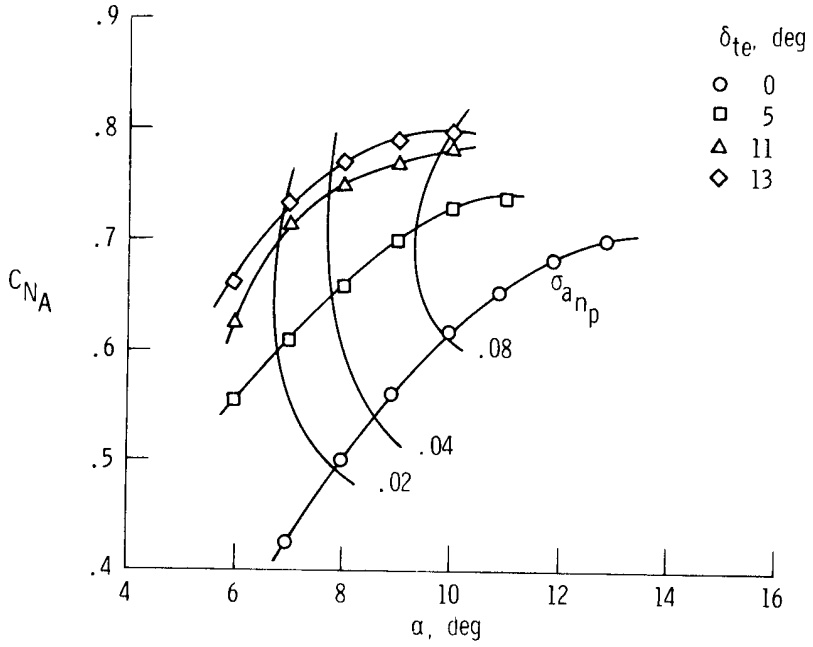

(c) $\delta_{le} = 3°$, selected δ_{te} positions.

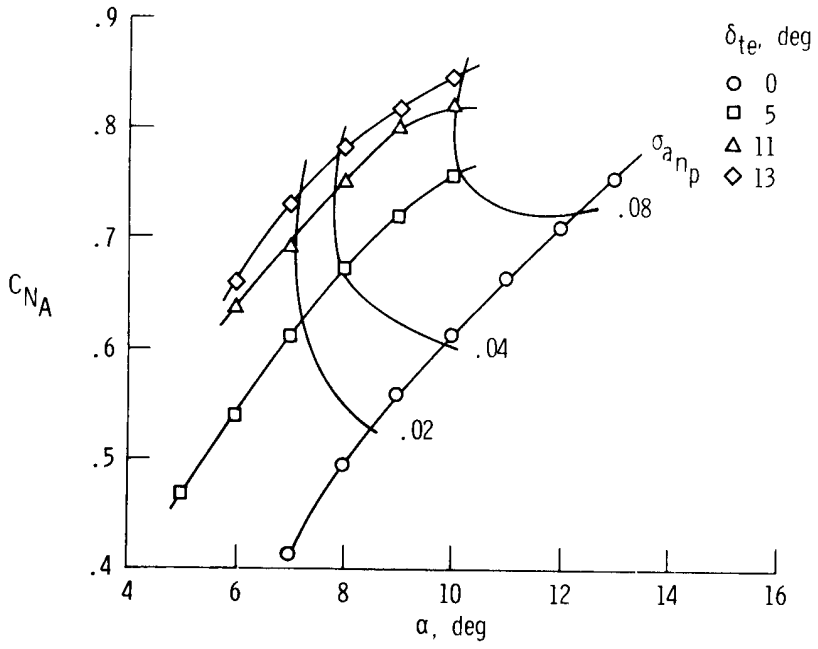

(d) $\delta_{le} = 7°$, selected δ_{te} positions.

Figure 12. Continued.

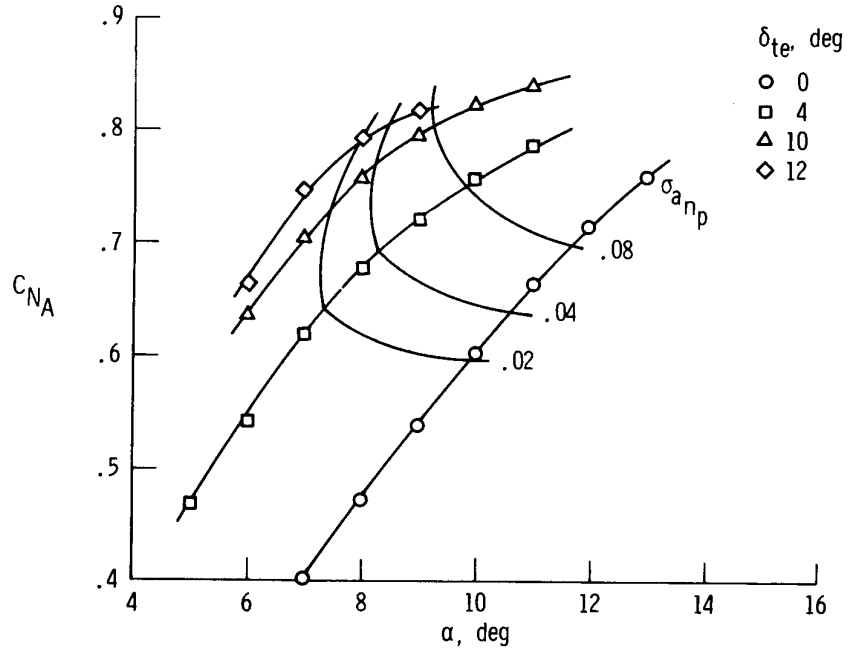

(e) $\delta_{le} = 11°$, selected δ_{te} positions.

Figure 12. Concluded.

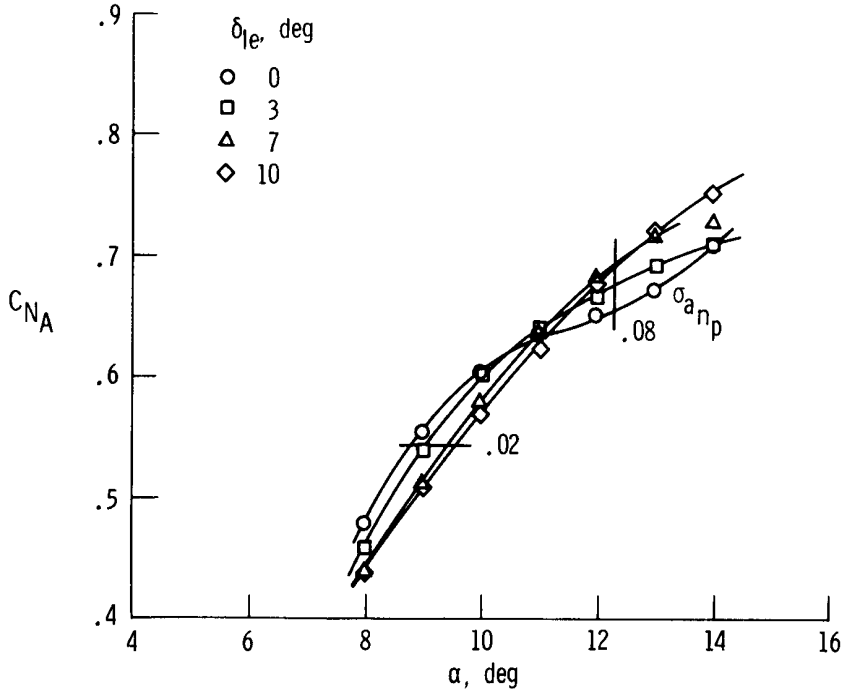

(a) Selected δ_{le} positions, $\delta_{te} = 0°$.

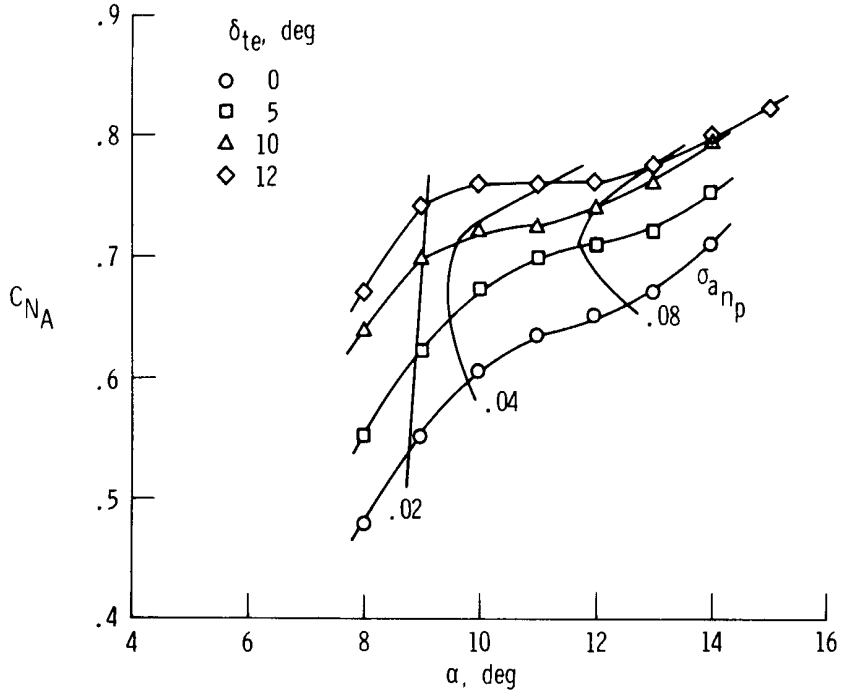

(b) $\delta_{le} = 0°$, selected δ_{te} positions.

Figure 13. Effect of wing-flap deflection on the variation of airplane normal-force coefficient with angle of attack at $M \approx 0.89$. $q \approx 13,400$ N/m^2 (280 lb/ft^2).

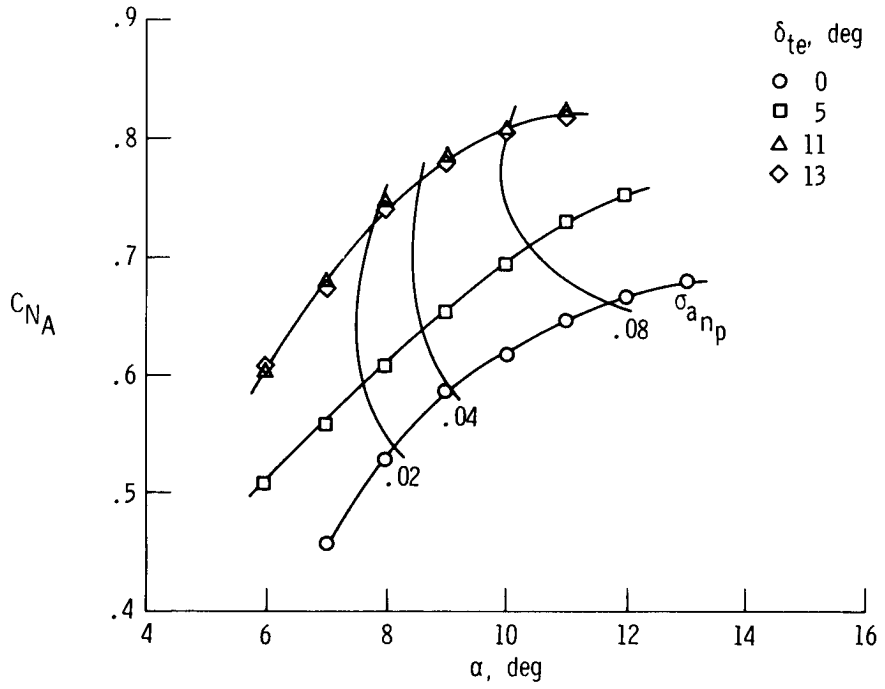

(c) $\delta_{le} = 3°$, selected δ_{te} positions.

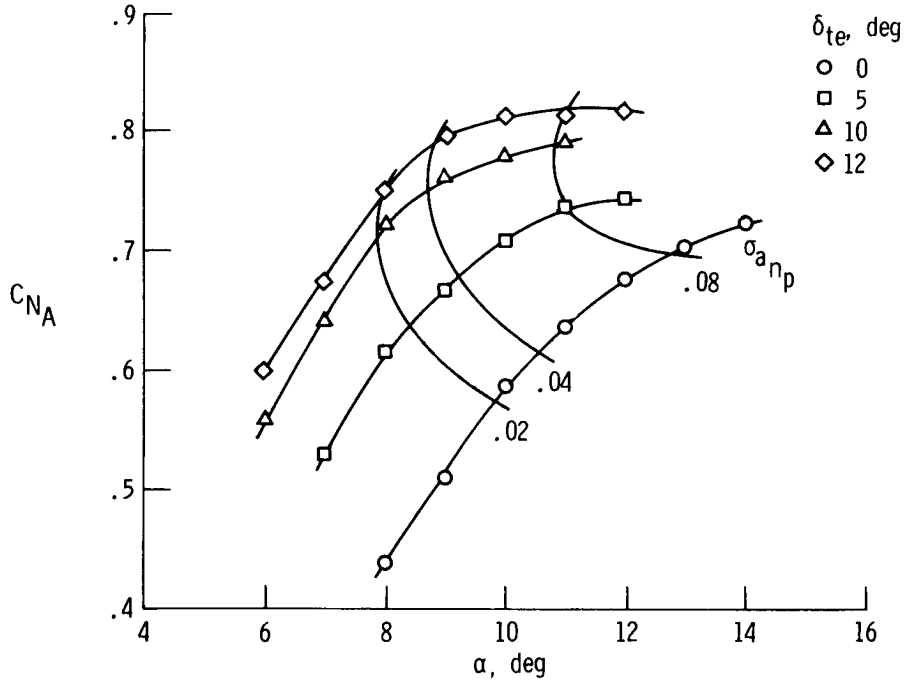

(d) $\delta_{le} = 7°$, selected δ_{te} positions.

Figure 13. Continued.

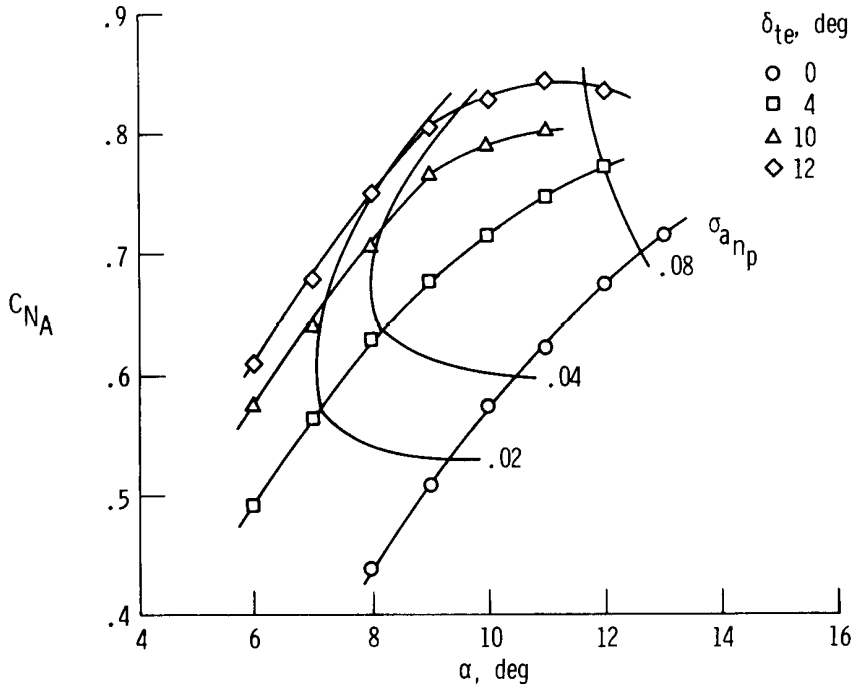

(e) $\delta_{le} = 11°$, selected δ_{te} positions.

Figure 13. Concluded.

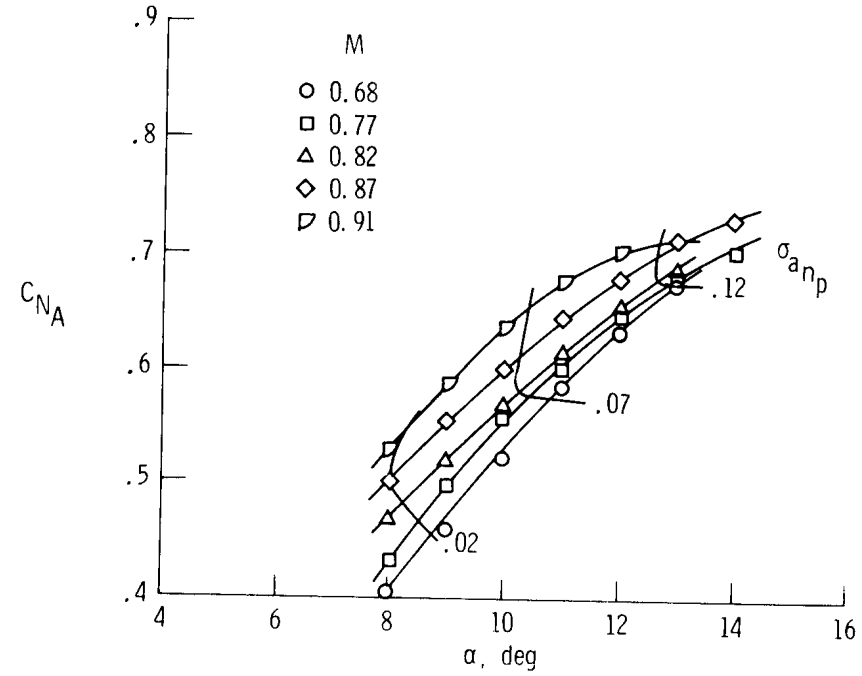

(a) Clean configuration.

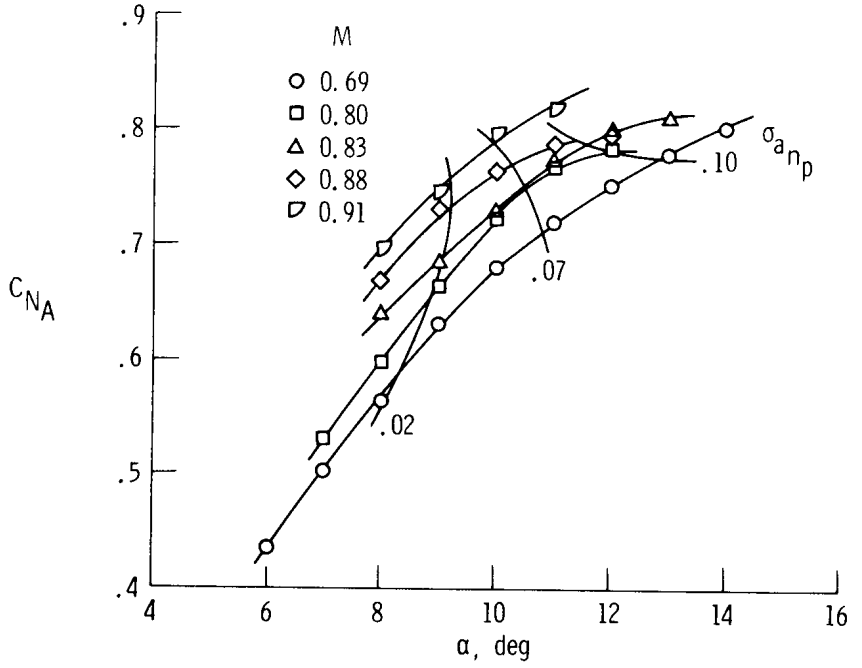

(b) $\delta_{le} = 4°$, $\delta_{te} = 10°$.

Figure 14. Variation of airplane normal-force coefficient with angle of attack at various Mach numbers. $q \approx 13,400$ N/m^2 (280 lb/ft^2).

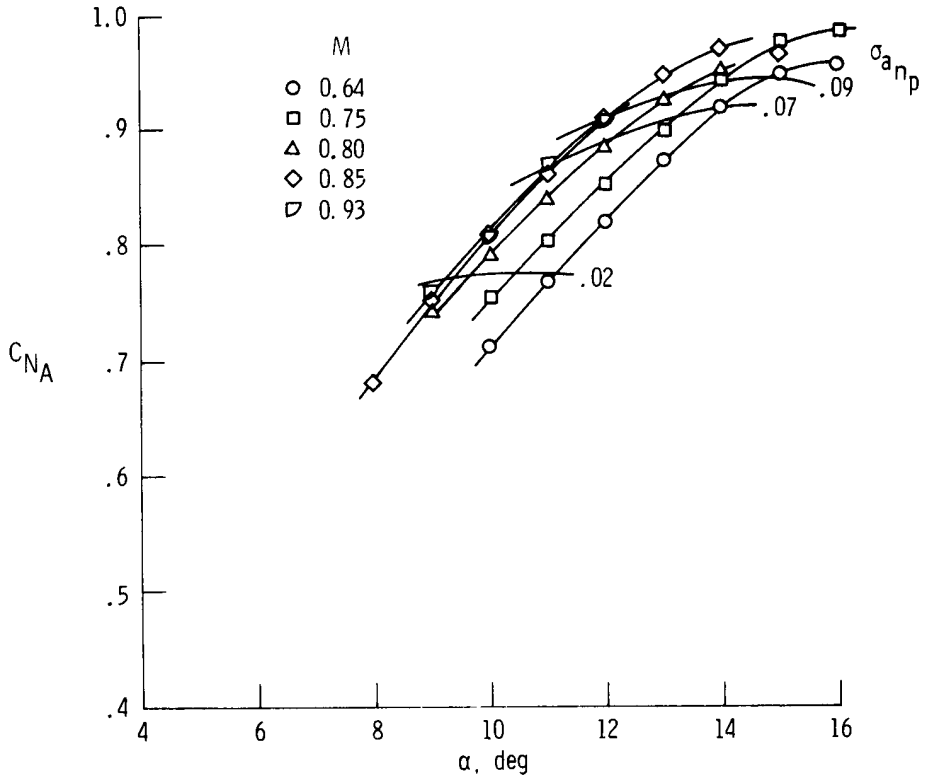

(c) $\delta_{le} = 12°$, $\delta_{te} = 13°$.

Figure 14. Concluded.

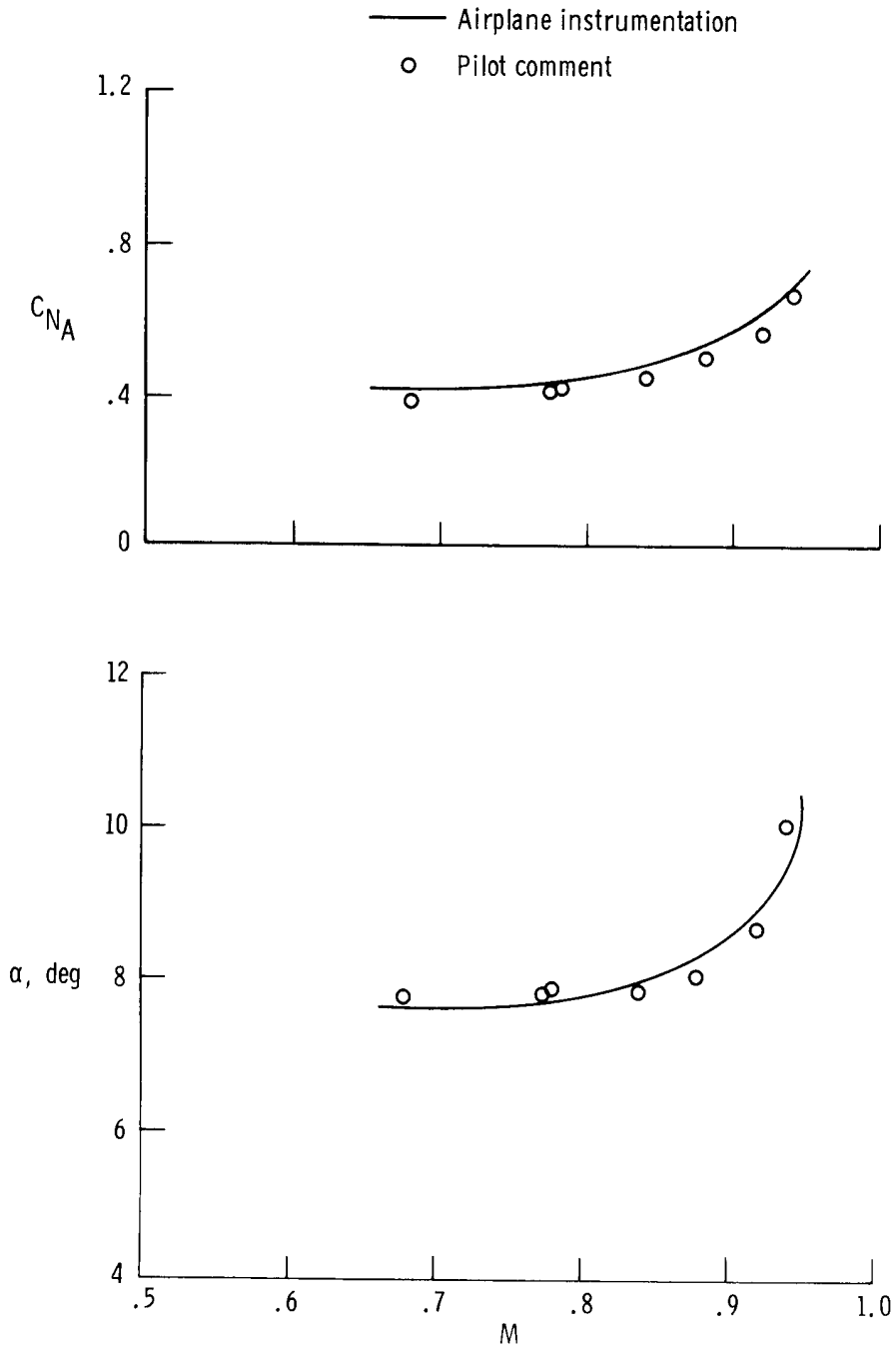

Figure 15. Comparison of buffet onset determined by pilot comment and airplane instrumentation. Clean configuration.

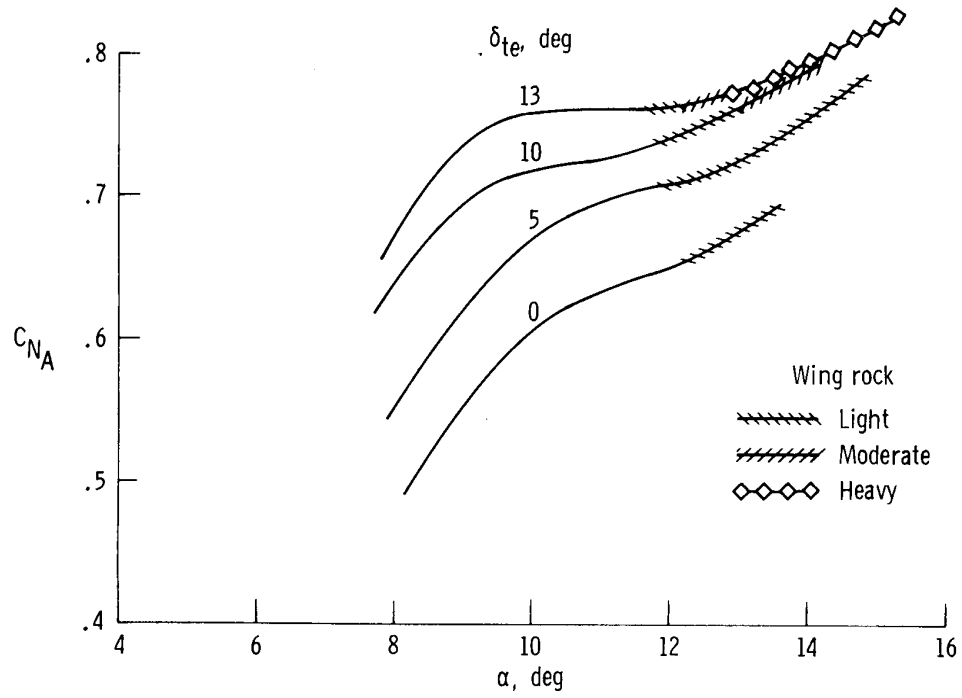

(a) $\delta_{le} = 0°$.

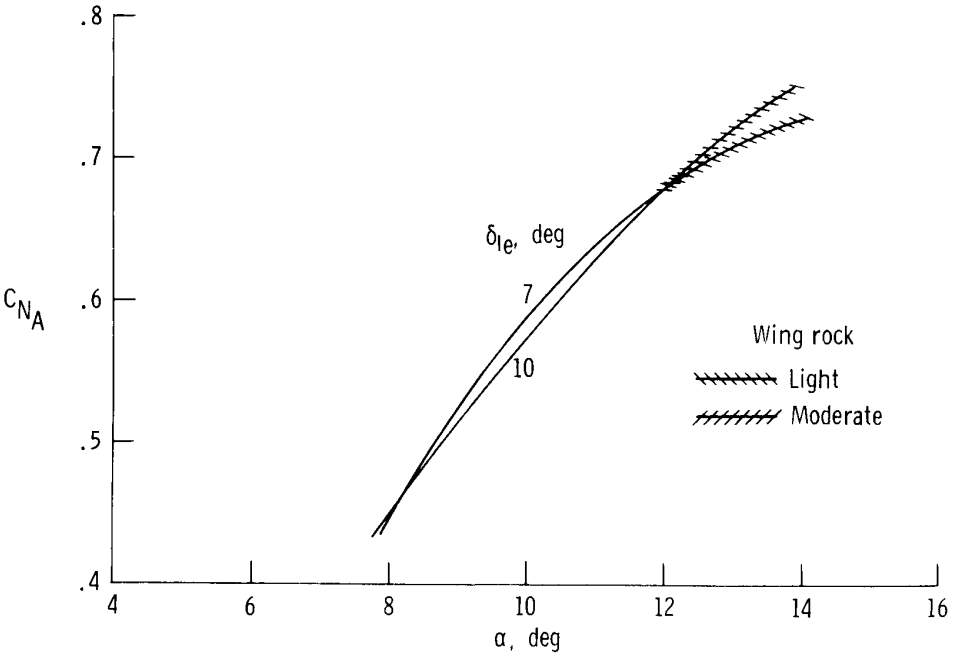

(b) $\delta_{te} = 0°$.

Figure 16. Typical lift curves showing wing-rock regions. $M \approx 0.89$.